Quasibrittle fracture scaling and size effect

Materials and Structures / Matériaux & Constructions, Vol **37**, January-February 2004

Quasibrittle fracture scaling and size effect

By RILEM Technical Committee Quasibrittle Fracture Scaling
Z. P. Bažant (chairman), B. I. G. Barr, R. de Borst, S. Burtscher, O. Buyukozturk, I. Carol, A. Carpinteri, B. Chiaia, J. P. Dempsey, M. Elices, G. Ferro, R. Gettu, V. S. Gopalaratnam, , C. Huet, M. Jirásek, S. L. McCabe, H. Mihashi, K. M. Nemati, J. Planas, P. Prat, K. Rokugo, P. Rossi, V. E. Saouma, F.-J. Ulm, M. van Vliet, J. L. Vítek, K. Willam, Y. Xi

Paper received: 26th August 2003

ABSTRACT

The report attempts a broad review of the problem of size effect or scaling of failure, which has recently come to the forefront of attention because of its importance for concrete and geotechnical engineering, geomechanics, arctic ice engineering, as well as in designing large load-bearing parts made of advanced ceramics and composites, e.g. for aircraft or ships. First the main results of Weibull statistical theory of random strength are briefly summarized and its applicability and limitations described. In this theory as well as plasticity, elasticity with a strength limit, and linear elastic fracture mechanics (LEFM), the size effect is a simple power law because no characteristic size or length is present. Attention is then focused on the deterministic size effect in quasibrittle materials which, because of the existence of a non-negligible material length characterizing the size of the fracture process zone, represents the bridging between the simple power-law size effects of plasticity and of LEFM. The energetic theory of quasibrittle size effect in the bridging region is explained and then a host of recent refinements, extensions and ramifications are discussed. Comments on other types of size effect, including that which might be associated with the fractal geometry of fracture, are also made. The historical development of the size effect theories is outlined and the recent trends of research are emphasized.

1 INTRODUCTION

The size effect is a problem of scaling, which is central to every physical theory. In fluid mechanics research, the problem of scaling continuously played a prominent role for over a hundred years. In solid mechanics research, though, the attention to scaling had many interruptions and became intense only during the last decade.

Not surprisingly, the modern studies of nonclassical size effect, begun in the 1970s, were stimulated by the problems concrete structures, for which there inevitably is a large gap between the scales of large structures (e.g. dams, reactor containments, bridges) and of laboratory tests. This gap involves in such structures about one order of magnitude (even in the rare cases when a full scale test is carried out, it is impossible to acquire a sufficient statistical basis on the full scale).

The question of size effect recently became a crucial consideration in the efforts to use advanced fiber composites and sandwiches for large ship hulls, bulkheads, decks, stacks and masts, as well as for large load-bearing fuselage panels. The scaling problems are even greater in geotechnical engineering, arctic engineering, and geomechanics. In analyzing the safety of an excavation wall or a tunnel, the risk of a mountain slide, the risk of slip of a fault in the earth crust, or the force exerted on an oil platform in the Arctic by a moving mile-size ice floe, the scale jump from the laboratory spans many orders of magnitude.

In most of mechanical and aerospace engineering, on the other hand, the problem of scaling has

been less pressing because the structures or structural components can usually be tested at full size. It must be recognized, however, that even in that case the scaling implied by the theory must be correct. Scaling is the most fundamental characteristic of any physical theory. If the scaling properties of a theory are incorrect, the theory itself is incorrect.

The size effect on structural strength is understood as the effect of the characteristic structure size (dimension) D on the nominal strength σ_N of structure when geometrically similar structures are compared. The nominal stress (or strength, in case of maximum load) is defined as $\sigma_N = c_N P/bD$ or $c_N P/D^2$ for two- or three-dimensional similarity, respectively; P = load (or load parameter), b structure thickness, and c_N arbitrary coefficient chosen for convenience (normally $c_N = 1$). So σ_N is not real stress but a load parameter having the dimension of stress. The definition of D can be arbitrary (e.g. the beam depth or half-depth, the beam span, the diagonal dimension, etc.) because it does not matter for comparing geometrically similar structures.

The basic scaling laws in physics are power laws in terms of D, for which no characteristic size (or length) exists. The classical Weibull (1939) theory of statistical size effect caused by randomness of material strength is of this type. During the 1970s it was found that a major deterministic size effect, overwhelming the statistical size effect, can be caused by stress redistributions due to stable propagation of fracture or damage and the inherent energy release. The law of the deterministic size effect provides a way of bridging two different power laws applicable in two adjacent size ranges. The structure size at which this bridging transition occurs represents a characteristic size.

The material for which this new kind of size effect was identified first, and studied in the greatest depth and with the largest experimental effort by far, is concrete. In general, a size effect that bridges the small-scale power law for nonbrittle (plastic, ductile) behavior and the large-scale power law for brittle behavior signals the presence of a certain non-negligible characteristic length of the material. This length, which represents the quintessential property of quasibrittle materials, characterizes the typical size of material inhomogeneities or the fracture process zone (FPZ). Aside from concrete, other quasibrittle materials include rocks, cement mortars, ice (especially sea ice), consolidated snow, tough fiber composites and particulate composites, toughened ceramics, fiber-reinforced concretes, dental cements, bone and cartilage, biological shells, stiff clays, cemented sands, grouted soils, coal, paper, wood, wood particle board, various refractories and filled elastomers, as well as some special tough metal alloys. Keen interest in the size effect and scaling is now emerging for various 'high-tech' applications of these materials.

Quasibrittle behavior can be attained by creating or enhancing material inhomogeneities. Such behavior is desirable because it endows the structure made from a material incapable of plastic yielding with a significant energy absorption capability. Long ago, civil engineers subconsciously but cleverly engineered concrete structures to achieve and enhance quasibrittle characteristics. Most modern 'high-tech' materials achieve quasibrittle characteristics in much the same way—by means of inclusions, embedded reinforcement, and intentional microcracking (as in transformation toughening of ceramics, analogous to shrinkage microcracking of concrete). In effect, they emulate concrete.

In materials science, an inverse size effect spanning several orders of magnitude must be tackled in passing from normal laboratory tests of material strength to microelectronic components and micromechanisms. A material that follows linear elastic fracture mechanics (LEFM) on the scale of laboratory specimens of sizes from 1 to 10 cm may exhibit quasibrittle or even ductile (plastic) failure on the scale of 0.1 or 100 microns.

The purpose of this report is to present a brief review of the basic results and their history. For an in-depth review with several hundred literature references, the recent article by Bažant and Chen (1997) may be consulted. A full exposition of most of the material reviewed here is found in the recent book by Bažant and Planas (1998), henceforth simply referenced as [BP]. The problem of scale bridging in the micromechanics of materials, e.g., the relation of dislocation theory to continuum plasticity, is beyond the scope of this review (it is treated in this volume by Hutchinson).

2 HISTORY OF SIZE EFFECT UP TO WEIBULL

Speculations about the size effect can be traced back to Leonardo da Vinci (1500s) (Williams 1957). He observed that "among cords of equal thickness the longest is the least strong," and proposed that "a cord is so much stronger ... as it is shorter," implying inverse proportionality. A century later, Galileo Galilei (1638), the inventor of the concept of stress, argued that Leonardo's size effect cannot be true. He further discussed the effect of the size of an animal on the shape of its bones, remarking that bulkiness of bones is the weakness of the giants.

A major idea was spawned by Mariotte (1686). Based on his extensive experiments, he observed that "a long rope and a short one always support the same weight unless that in a long rope there may happen to be some faulty place in which it will break sooner than in a shorter", and proposed the principle of "the inequality of matter whose absolute resistance is less in one place than another." In

other words, the larger the structure, the greater is the probability of encountering in it an element of low strength. This is the basic idea of the statistical theory of size effect.

Despite no lack of attention, not much progress was achieved for two and half centuries, until the remarkable work of Griffith (1921), the founder of fracture mechanics. He showed experimentally that the nominal strength of glass fibers was raised from 292 MPa to 3.39 GPa when the diameter decreased from 107 μm to 3.3 μm, and concluded that "the weakness of isotropic solids...is due to the presence of discontinuities or flaws... The effective strength of technical materials could be increased 10 or 20 times at least if these flaws could be eliminated." In Griffith's view, however, the flaws or cracks at the moment of failure were still only microscopic; their random distribution controlled the macroscopic strength of the material but did not invalidate the concept of strength. Thus, Griffith discovered the physical basis of Mariotte's statistical idea but not a new kind of size effect.

The statistical theory of size effect began to emerge after Peirce (1926) formulated the weakest-link model for a chain and introduced the extreme value statistics which was originated by Tippett (1925), Fischer and Tippett (1928), and Fréchet (1927), and refined by von Mises (1936) and others (see also Freudenthal 1968, Freudenthal and Gumbell 1956, Selected Papers 1981, Evans 1978). The capstone of the statistical theory was laid by Weibull (1939) (also Weibull 1949, 1951, 1956). On a heuristic and experimental basis, he concluded that the tail distribution of low strength values with an extremely small probability could not be adequately represented by any of the previously known distributions. He introduced what came to be known as the Weibull distribution, which gives the probability of a small material element as a power law of the strength difference from a finite or zero threshold. Others (e.g., Freudenthal 1968; Selected Papers 1981) later offered a theoretical justification by means of a statistical distribution of microscopic flaws or microcracks. Refinement of applications to metals and ceramics (fatigue embrittlement, cleavage toughness of steels at low and brittle-ductile transition temperatures, evaluation of scatter of fracture toughness data) has continued until today (e.g. Evans 1978, Beremin 1983, Ruggieri and Dodds 1996, Lei et al. 1998).

Most subsequent studies of the statistical theory of size effect dealt basically with refinements and applications of Weibull's theory to fatigue embrittled metals and to ceramics (e.g., Kittl and Diaz 1988, 1990). Applications to concrete, where the size effect were of the greatest concern, have been studied by Zaitsev and Wittmann 1974; Mihashi and Zaitsev 1981, Wittmann and Zaitsev 1981, Zech and Wittmann 1977, Mihashi 1983; Mihashi and Izumi 1977, Carpinteri 1986, 1989), and others.

Until about 1985, most mechanicians paid almost no attention to the possibility of a deterministic size effect. Whenever a size effect was detected in tests, it was automatically assumed to be statistical, and thus its study was supposed to belong to statisticians rather than mechanicians. The reason probably was that no size effect is exhibited by the classical continuum mechanics in which the failure criterion is written in terms of stresses and strains (elasticity with strength limit, plasticity and viscoplasticity, as well as fracture mechanics of bodies containing only microscopic cracks or flaws); Bažant (1993). The subject was not even mentioned by S.P. Timoshenko in 1953 in his monumental History of the Strength of Materials.

The attitude, however, changed drastically in the 1980s. In consequence of the well-funded research in concrete structures for nuclear power plants, theories exhibiting a deterministic size effect have been developed. We will discuss it later.

3 POWER SCALING AND THE CASE OF NO SIZE EFFECT

It is proper to explain first the simple scaling applicable to all physical systems that involve no characteristic length. Let us consider geometrically similar systems, for example the beams shown in Fig. 1a, and seek to deduce the response Y (e.g., the maximum stress or the maximum deflection) as a function of the characteristic size (dimension) D of the structure. We choose a certain reference size D_0 and denote the corresponding response as Y_0. For a geometrically similar structure of an arbitrary size D, the response can be expressed as $Y = Y_0 f(D/D_0)$ where f is a dimensionless function of a dimensionless argument, describing the scaling law. For example, for sizes D_1 and D_2 we have $Y_1 = Y_0 f(D_1/D_0)$ and $Y_2 = Y_0 f(D_2/D_0)$. However, since there is no characteristic length, we can also take D_1 as the reference size and write $Y_2 = Y_1 f(D_2/D_1)$. Consequently, the equation

$$f\left(\frac{D_2}{D_1}\right) f\left(\frac{D_1}{D_0}\right) = f\left(\frac{D_2}{D_0}\right) \qquad (1)$$

must hold for any combination of sizes D_0, D_1 and D_2. This is a functional equation for the unknown scaling function f. Any possible solution must have the form of a power law

$$f\left(\frac{D}{D_0}\right) = \left(\frac{D}{D_0}\right)^s \qquad (2)$$

where s is an arbitrary but fixed exponent.

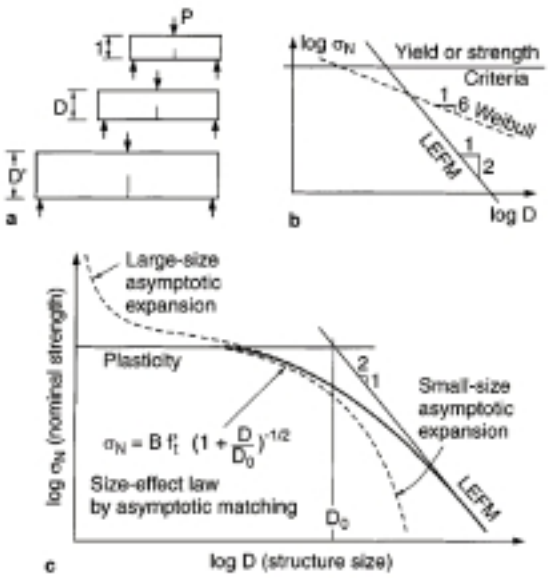

Fig. 1 – (a) Geometrically similar structures of different sizes, (b) power scaling laws, (c) size effect law for quasibrittle failures bridging the power law of plasticity (horizontal asymptote) and the power law of LEFM (inclined asymptote).

On the other hand, when for instance $f(D/D_0) = \log(D/D_0)$, Eq. (1) is not satisfied. So, the logarithmic scaling could be possible only if the system possessed a characteristic length and a change of the reference size implied a change of the scaling function f.

The power scaling must apply for every physical theory in which there is no characteristic length. In solid mechanics such failure theories include elasticity with a strength limit, elasto-plasticity, viscoplasticity as well as LEFM (for which the FPZ is assumed shrunken into a point).

To determine exponent s, the failure criterion of the material must be taken into account. For elasticity with a strength limit (strength theory), or plasticity (or elasto-plasticity) with a yield surface expressed in terms of stresses or strains, or both, one finds that $s = 0$ when response Y represents the stress or strain (for example the maximum stress, or the stress at certain homologous points, or the nominal stress at failure); Bažant (1993). Thus, if there is no characteristic dimension, all geometrically similar structures of different sizes must fail at the same nominal stress. By convention, this came to be known as the case of *no size effect*.

In LEFM, on the other hand, $s = -1/2$, provided that the geometrically similar structures with geometrically similar cracks or notches are considered. This may be generally demonstrated with the help of Rice's J-integral (Bažant, 1993).

If $\log \sigma_N$ is plotted versus $\log D$, the power law is a straight line (Fig. 1b). For plasticity, or elasticity with a strength limit, the exponent of the power law vanishes, i.e., the slope of this line is 0. For LEFM, the slope is $-1/2$. An emerging 'hot' subject is the quasibrittle materials and structures, for which the size effect bridges these two power laws.

4 WEIBULL STATISTICAL SIZE EFFECT

The classical theory of size effect has been statistical. Three-dimensional continuous generalization of the weakest link model for the failure of a chain of links of random strength (Fig. 2a) leads to the distribution

$$P_f(\sigma_N) = 1 - \exp\left[-\int_V c[\boldsymbol{\sigma}(\boldsymbol{x}), \sigma_N)]dV(\boldsymbol{x})\right] \tag{3}$$

which represents the probability that a structure that fails as soon as macroscopic fracture initiates from a microcrack (or a some flaw) somewhere in the structure; σ = stress tensor field induced by the load that corresponds to the nominal stress σ_N, $\boldsymbol{x}$ = coordinate vector, V = volume of structure, and $c(\boldsymbol{\sigma})$ = function giving the spatial concentration of failure probability of the material (= $V_r^{-1}\times$ failure probability of material representative volume V_r) (Freudenthal 1968); $c(\boldsymbol{\sigma}) \approx \sum_i P_1(\sigma_i)/V_0$ where σ_i = principal stresses (i = 1,2,3) and $P_1(\sigma)$ = failure probability (cumulative) of the smallest possible test specimen of volume V_0 (or representative volume of the material) subjected to uniaxial tensile stress σ;

$$P_1(\sigma) = \left\langle \frac{\sigma - \sigma_u}{s_0} \right\rangle^m \tag{4}$$

(Weibull 1939) where m, s_0, σ_1 = material constants (m = Weibull modulus, usually between 5 and 50; s_0 = scale parameter; σ_u = strength threshold, which may usually be taken as 0) and V_0 = reference volume understood as the volume of specimens on which $c(\sigma)$ was measured. For specimens under uniform uniaxial stress (and σ_u = 0), (3) and (4) lead to the following simple expressions for the mean and coefficient of variation of the nominal strength:

$$\overline{\sigma}_N = s_0\Gamma(1+m^{-1})(V_0/V)^{1/m} \tag{5}$$

$$\omega = \sqrt{\frac{\Gamma(1+2m^{-1})}{\Gamma^2(1+m^{-1})} - 1} \tag{6}$$

where Γ is the gamma function. Since ω depends only on m, it is often used for determining m from the observed statistical scatter of strength of identical test specimens. The expression for $\overline{\sigma}_N$ includes the effect of volume V which depends on size D. In general, for structures with nonuniform multidimensional stress, the size effect of Weibull theory (for $\sigma_u \approx 0$) is of the type:

$$\overline{\sigma}_N \propto D^{-n_d/m} \tag{7}$$

where n_d = 1, 2 or 3 for uni-, two- or three-dimensional similarity.

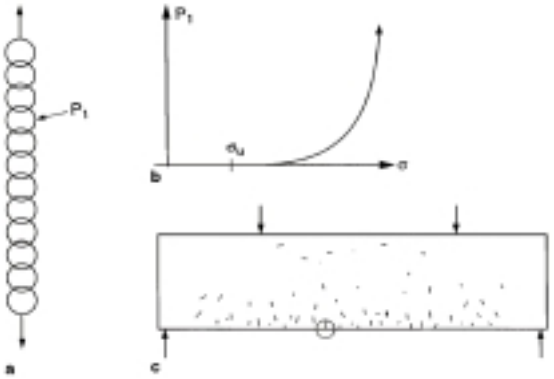

Fig. 2 – (a) Chain with many links of random strength, (b) failure probability of a small element, (c) structure with many microcracks of different probabilities to become critical.

In view of (5), the value $\sigma_W = \sigma_N (V/V_0)^{1/m}$ for a uniformly stressed specimen can be adopted as a size-independent stress measure called the Weibull stress. Taking this viewpoint, Beremin (1983) proposed taking into account the nonuniform stress in a large crack-tip plastic zone by the so-called Weibull stress:

$$\sigma_W = \left(\sum_i {\sigma_I}_i^m \frac{V_i}{V_0} \right)^{1/m} \qquad (8)$$

where V_i ($i = 1, 2, \ldots N_W$) are elements of the plastic zone having maximum principal stress σ_{Ii}. Ruggieri and Dodds (1996) replaced the sum in (5) by an integral; see also Lei et al. (1998). Eq. (8), however, considers only the crack-tip plastic zone whose size is almost independent of D. Consequently, Eq. (8) is applicable only if the crack at the moment of failure is not yet macroscopic, still being negligible compared to structural dimensions.

As far as quasibrittle structures are concerned, applications of the classical Weibull theory face a number of serious objections:

1. The fact that in (7) the size effect is a power law implies the absence of any characteristic length. But this cannot be true if the material contains sizable inhomogeneities.

2. The energy release due to stress redistributions caused by macroscopic FPZ or stable crack growth before the peak load, P_{max}, gives rise to a deterministic size effect which is ignored. Thus the Weibull theory is valid only if the structure fails as soon as a microscopic crack becomes macroscopic.

3. According to the classical Weibull theory, every structure would be mathematically equivalent to a uniaxially stressed bar (or chain, Fig. 2), which means that no information on the structural geometry and failure mechanism is taken into account.

4. The size effect differences between two- and three-dimensional similarity (n_d = 2 or 3) are predicted much too large.

5. Many tests of quasibrittle materials (e.g., diagonal shear failure of reinforced concrete beams) show a much stronger size effect than predicted by Weibull theory ([BP], and the review in Bažant 1997a).

6. The classical theory neglects the spatial correlations of material failure probabilities of neighboring elements caused by nonlocal properties of damage evolution (while generalizations based on some phenomenological load-sharing hypotheses have been divorced from mechanics).

7. When (5) is fit to the test data on statistical scatter for specimens of one size (V = const.), and when (7) is fit to the mean test data on the effect of size or V (of unnotched plain concrete specimens), the optimum values of Weibull exponent m are very different, namely $m = 12$ and $m = 24$, respectively (Bažant and Novák 2000c). If the theory were applicable, these value would have to coincide.

In view of these limitations, among concrete structures Weibull theory appears applicable to some extremely thick plain (unreinforced) structures, e.g., the flexure of an arch dam acting as a horizontal beam (but not for vertical bending of arch dams nor gravity dams because large vertical compressive stresses cause long cracks to grow stably before the maximum load). Most other plain concrete structures are not thick enough to prevent the deterministic size effect from dominating. Steel or fiber reinforcement prevents it as well.

5 QUASIBRITTLE SIZE EFFECT BRIDGING PLASTICITY AND LEFM, AND ITS HISTORY

Quasibrittle materials are materials that (1) are incapable of purely plastic deformations and (2), in normal use, have an FPZ which is not negligible compared to structure size D. The concept of quasi-brittleness is not absolute but *relative*, depending on D. For a large enough D, every quasibrittle structure becomes brittle, i.e., follows LEFM, except that crack initiation is governed by material strength (which itself is determined by fracture behavior of microscopic flaws in the FPZ, as in brittle ceramics or fatigue-embrittled steel). For small enough D, every quasibrittle structure is equivalent to an elastic body with a perfectly plastic crack (as proven in Bažant 2002a) and follows the theory of plasticity, although the size D for which such plastic

behavior is attained may represent an abstract theoretical extrapolation in which D is smaller than the inhomogeneity size of the material. All brittle materials (i.e., materials in which the crack growth is governed by LEFM) become quasibrittle on a small enough scale (e.g., a fine-grained ceramic, brittle for $D > 1$ mm, may be quasibrittle for $D \approx 1$ μm), and all quasibrittle materials become perfectly brittle on a large enough scale (e.g., concrete with normal-size aggregate on the scale of a large gravity dam, sea ice on the scale of 100 m, or jointed rock mass, with joints at 10 m separation, on the scale of a whole mountain, exceeding 1 km).

While plasticity alone, as well as LEFM alone, possesses no characteristic length, the combination of both, which must be considered for the bridging of plasticity and LEFM, does. Irwin (1958) studied the size ℓ_p of the plastic zone that forms ahead of a crack tip. He derived a rough estimate $\ell_p \approx K_I^2/\pi\sigma_0^2$, where K_I is the mode-I stress intensity factor and σ_0 is the material strength or yield limit. At incipient crack propagation under plane stress, K_I is equal to the fracture toughness, $K_{IC} = \sqrt{EG_F}$, where E is Young's modulus and G_F is the fracture energy. This motivates the definition of a characteristic length (material length)

$$\ell_0 = \frac{EG_F}{\sigma_0^2} \tag{9}$$

which approximately characterizes the size of the FPZ in quasibrittle materials. So the key to the deterministic quasibrittle size effect is a combination of the concept of strength or yield with fracture mechanics. In dynamics, this further implies the existence of a characteristic time (material time):

$$\tau_0 = \ell_0/v \tag{10}$$

representing the time a wave of velocity v takes to propagate the distance ℓ_0.

After LEFM was first applied to concrete (Kaplan 1961), it was found to disagree with test results (Kesler et al. 1971; Leicester 1969; Walsh 1972, 1976). Leicester (1969) tested geometrically similar notched beams of different sizes, fit the results by a power law, $\sigma_N \propto D^{-n}$, and observed that the optimum n was less than $1/2$, the value required by LEFM. The power law with a reduced exponent of course fits the test data in the central part of the transitional size range well but does not provide the bridging of the ductile and LEFM size effects. It was tried to explain the reduced exponent value by notches of a finite angle, which however is objectionable for two reasons: (i) notches of a finite angle cannot propagate (rather, a crack must emanate from the notch tip), (ii) the singular stress field of finite-angle notches gives a zero flux of energy into the notch tip. Same as Weibull theory, Leicester's power law also implied nonexistence of a characteristic length (see Bažant and Chen, 1997, Eqs. 1-3), which cannot be the case for concrete due to the large size of its inhomogeneities. More extensive tests of notched geometrically similar concrete beams of different sizes were carried out by Walsh (172, 1976). Although he did not attempt a mathematical formulation, he was first to make the doubly logarithmic plot of nominal strength versus size and observe that it was transitional between plasticity and LEFM.

An important advance was made by Hillerborg et al. (1976) (also Petersson 1981). Inspired by the softening and plastic FPZ models of Barenblatt (1959, 1962) and Dugdale (1960), they formulated the cohesive (or fictitious) crack model characterized by a softening stress-displacement law for the crack opening and showed by finite element calculations that the failures of unnotched plain concrete beams in bending exhibit a deterministic size effect, in agreement with tests of the modulus of rupture.

Analyzing distributed (smeared) cracking damage, Bažant(1976) demonstrated that its localization into a crack band engenders a deterministic size effect on the postpeak deflections and energy dissipation of structures. The effect of the crack band is approximately equivalent to that of a long fracture with a sizable FPZ at the tip. Subsequently, using an approximate energy release analysis, Bažant (1984) derived for the quasibrittle size effect in structures failing after large stable crack growth the following approximate size effect law:

$$\sigma_N = B\sigma_0 \left(1 + \frac{D}{D_0}\right)^{-1/2} + \sigma_R \tag{11}$$

or more generally:

$$\sigma_N = B\sigma_0 \left[1 + \left(\frac{D}{D_0}\right)^r\right]^{-1/2r} + \sigma_R \tag{12}$$

in which r, B = positive dimensionless constants; D_0 = constant representing the transitional size (at which the power laws of plasticity and LEFM intersect); both D_0 and B depend on the structure geometry (shape). Usually constant $\sigma_R = 0$, except when there is a residual crack-bridging stress σ_r outside the FPZ (as in fiber composites), or when at large sizes some plastic mechanism acting in parallel emerges and becomes dominant (as in the Brazilian split-cylinder test).

Eq. (11) was shown to be closely followed by the numerical results for the crack band model (Bažant 1976, Bažant and Oh 1983), as well as for the nonlocal continuum damage models, which are capable of realistically simulating the localization of strain-softening damage and avoiding spurious mesh sensitivity.

Beginning in the mid 1980s, the interest in the quasibrittle size effect of concrete structures surged

enormously and many researchers made noteworthy contributions; to name but a few: Planas and Elices (1988, 1989, 1993), Petersson (1981), and Carpinteri (1986). The size effect has recently become a major theme at conferences on concrete fracture (Bažant, ed., 1992, Mihashi et al., eds., 1994, Wittmann, ed., 1995, Carpinteri, ed., 1996, Mihashi and Rokugo, eds., 1998, Bažant and Rajapakse, 1999).

Measurements of the size effect on P_{max} were shown to offer a simple way to determine the fracture characteristics of quasibrittle materials, including the fracture energy, the effective FPZ length, and the (geometry dependent) R-curve.

6 SIZE EFFECT MECHANISM: STRESS REDISTRIBUTION AND ENERGY RELEASE

Let us now describe the gist of the deterministic quasibrittle size effect. LEFM applies when the FPZ is negligibly small compared to structural dimension D and can be considered as a point. Thus the LEFM solutions can obtained by methods of elasticity. The salient characteristic of quasibrittle materials is that there exists a sizable FPZ with distributed cracking or other softening damage that is not negligibly small compared to structural dimension D. This makes the problem nonlinear, although approximately equivalent LEFM solutions can be applied unless FPZ reaches near the structure boundaries.

The existence of a large FPZ means that the distance between the tip of the actual (traction-free) crack and the tip of the equivalent LEFM crack at P_{max} is equal to a certain characteristic length c_f (roughly one half of the FPZ size) that is not negligible compared to D. An "equivalent LEFM" solution may be rigorously defined as the solution for which the load-point stiffness is the same as the actual stiffness (Bažant and Planas 1998); this occurs when the tip of the LEFM crack is placed approximately in the center of FPZ. The large FPZ size causes a non-negligible macroscopic stress redistribution with energy release from the structure.

With respect to the fracture length a_0 (distance from the mouth of notch or crack to the beginning of the FPZ), two basic cases may now be distinguished: (i) $a_0 = 0$, which means that P_{max} occurs at the initiation of macroscopic fracture propagation, and (ii) a_0 is finite and not negligible compared to D, which means that P_{max} occurs after large stable fracture growth.

6.1 Scaling for failure at crack initiation

An example of the first case is the modulus of rupture test, which consists in the bending of a simply supported beam of span L with a rectangular cross section of depth D and width b, subjected to concentrated load P. The maximum load is not decided by the stress $\sigma_1 = 3PL/2bD^2 = (3L/2D)\sigma_N$ at the tensile face, but by the stress value $\bar{\sigma}$ roughly at distance c_f from the tensile face (which is roughly at the middle of FPZ). Approximately, $\bar{\sigma} = \sigma_1 - \sigma_1' c_f$ where $\sigma' = 2\sigma_1/D$ = stress gradient. Setting $\bar{\sigma} = f_t'$ = tensile strength of the material, we have $(3L/2D)\sigma_N(1 - 2c_f/D) = f_t'$, which gives $\sigma_N = \sigma_0/(1 - D_b/D)$, in which $\sigma_0 = (2D/3L)f_t'$ and $D_b = 2c_f$ (= thickness of the boundary layer of cracking) are constants because the ratio D/L is constant for geometrically similar structures. This expression for σ_N, however, is unacceptable for $D \leq D_b$. But since the derivation is valid only for small enough c_f/D (i.e., up to the first-order term of the asymptotic expansion of σ_N in terms of $1/D$), one may replace it by the following asymptotically equivalent size effect formula:

$$\sigma_N = \sigma_0 \left(1 + \frac{rD_b}{D}\right)^{1/r} \tag{13}$$

which happens to be acceptable for the entire range of D (including $D \to 0$); r is any positive constant. The values $r = 1$ or 2 have been used for concrete (Bažant 1998), while $r \approx 1.47$ is optimum according to Bažant and Novák's (2000a) latest analysis of test data.

6.2 Scaling for failures with a long crack or notch

Let us now give a simple explanation of the second case of structures failing only after stable formation of large cracks, or notched fracture specimens. Failures of this type, exhibiting a strong size effect ([BP], Bažant 1996, Walraven 1995, Iguro et al. 1985, Shioya and Akiyama 1995, Bažant and Kazemi 1991, Gettu et al. 1990, Marti 1989) are typical of reinforced concrete structures or fiber composites (Bažant, Li and Daniel 1986, Wisnom 1992), and are also exhibited by some unreinforced structures (e.g., dams, due to the effect of vertical compression, or floating ice plates in the Arctic). Consider the rectangular panel in Fig. 3, which is initially under a uniform stress equal to σ_N. Introduction of a crack of length a with a FPZ of a certain length and width h may be approximately imagined to relieve the stress, and thus release the strain energy, from the shaded triangles on the flanks of the crack band shown in Fig. 3. The slope k of the effective boundary of the stress relief zone need not be determined; what is important is that k is independent of the size D.

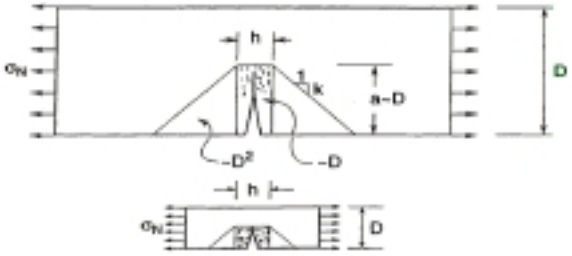

Fig. 3 – Approximate zones of stress relief due to fracture.

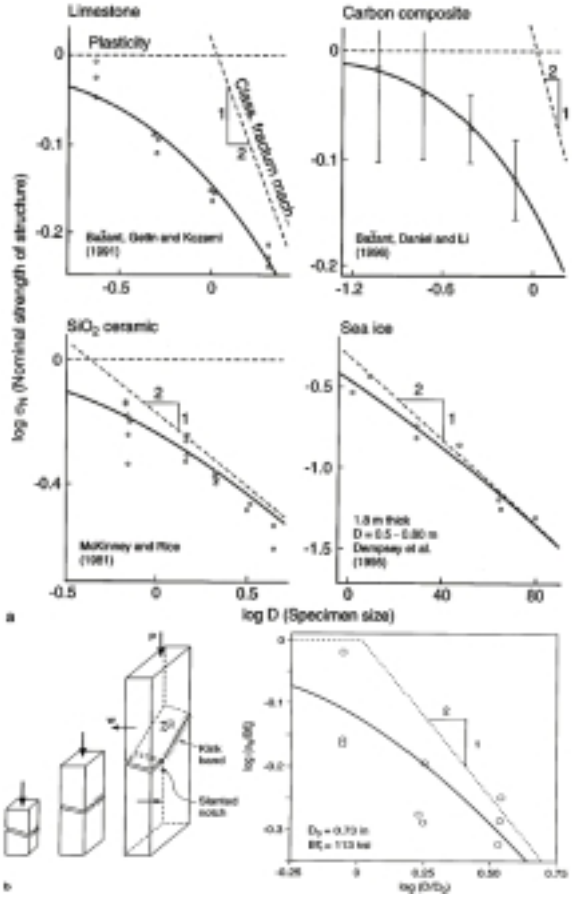

Fig. 4 – (a) Comparisons of size effect law with Mode I test data obtained by various investigators using notched specimens of different materials, (b) size effect in compression kink-band failures of geometrically similar notched carbon-PEEK specimens (after Bažant et al. 1999).

For the usual ranges of interest, the length of the crack at maximum load may normally be assumed approximately proportional to the structure size D while the size h of the FPZ is essentially a constant, related to the inhomogeneity size in the material. This has been verified for many cases by experiments (showing similar failure modes for small and large specimens) and finite element solutions based on crack band, cohesive or nonlocal models.

The stress reduction in the triangular zones of areas $ka^2/2$ (Fig. 3) causes (for the case $b = 1$) the energy release $U_a = 2 \times (ka^2/2)\sigma_N^2/2E$. The stress drop within the crack band of width h causes further energy release $U_b = ha\sigma_N^2/2E$. The total energy dissipated by the fracture is $W = aG_F$, where G_F is the fracture energy, a material property representing the energy dissipated per unit area of the fracture surface. Energy balance during static failure requires that $\partial(U_a + U_b)/\partial a = dW/da$. Setting $a = D(a/D)$ where a/D is approximately a constant if the failures for different structure sizes are geometrically similar, the solution of the last equation for σ_N yields Bažant's (1984) approximate size effect law in (11) with σ_R = 0 (Fig. 1c).

More rigorous derivations of this law, applicable to arbitrary structure geometry, have been given in terms of asymptotic analysis based equivalent LEFM (Bažant 1997b) or on Rice's path-independent J-integral (Bažant and Planas 1998). This law has also been verified by nonlocal finite element analysis, and by random particle (or discrete element) models. The experimental verifications, among which the earliest is found in the famous Walsh's (1972, 1976) tests of notched concrete beams, have by now become abundant (e.g. Fig. 4).

For very large sizes ($D \gg D_0$), the size effect law in (11) reduces to the power law $\sigma_N \propto D^{-1/2}$, which represents the size effect of LEFM (for geometrically similar large cracks) and corresponds to the inclined asymptote of slope $-1/2$ in Fig. 1c. For very small sizes ($D \ll D_0$), this law reduces to σ_N = const,, which corresponds to the horizontal asymptote and means that there is no size effect, as in plastic limit analysis.

The ratio $\beta = D/D_0$ is called the brittleness number of a structure. For $\beta \to \infty$ the structure is perfectly brittle (i.e. follows LEFM), in which case the size effect is the strongest possible, while for $\beta \to 0$ the structure is non-brittle (or ductile, plastic), in which case there is no size effect. Quasibrittle structures are those for which $0.1 \leq \beta \leq 10$, in which case the size effect represents a smooth transition (or interpolation) that bridges the power law size effects for the two asymptotic cases. The law (11) has the character of asymptotic matching and serves to provide the bridging of scales. In the quasibrittle range, the stress analysis is of course nonlinear, calling for the cohesive crack model or the crack band model (which are mutually almost equivalent), or some of the nonlocal damage models.

The meaning of the term quasibrittle is relative. If the size of a quasibrittle structure becomes sufficiently large compared to material inhomogeneities, the structure becomes perfectly brittle (for concrete structures, only the global fracture of a large dam is describable by LEFM), and if the size becomes sufficiently small, the structure becomes non-brittle (plastic, ductile) because the FPZ extends over the

whole cross section of the structure (thus a micromachine or a miniature electronic device made of silicone or fine-grained ceramic may be quasibrittle or non-brittle).

6.3 Size effect on postpeak softening and ductility

The plots of nominal stress versus the relative structure deflection (normalized so as to make the initial slope in Fig. 5 size independent) have, for small and large structures, the shapes indicated in Fig. 5. Apart from the size effect on P_{max}, there is also a size effect on the shape of the postpeak descending load-deflection curve. For small structures the postpeak curves descend slowly, for larger structures they are steeper, and for sufficiently large structures they may exhibit a snapback, that is, a change of slope from negative to positive. These structural size effects were analyzed for concrete structures by Carpinteri (1984), Carpinteri, Di Tommaso and Fanelli (1985), Carpinteri (1989a-e), and Carpinteri and Colombo (1989).

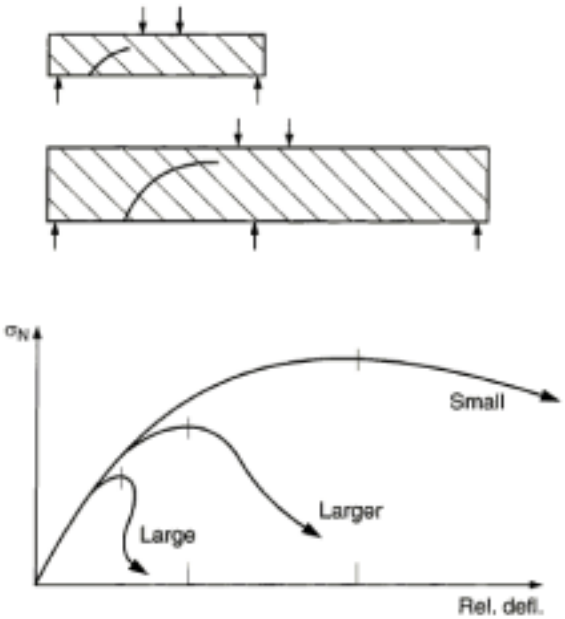

Fig. 5 – Load-deflection curves of quasibrittle structures of different sizes, scaled to the same initial slope.

If a structure is loaded under displacement control through an elastic device with spring constant C_s, it loses stability and fails at the point where the load-deflection diagram first attains the slope $-C_s$ (if ever); Fig. 5. The ratio of the deflection at these points to the elastic deflection characterizes the ductility of the structure. As apparent from the figure, small quasibrittle structures have a large ductility while large quasibrittle structures have small ductility.

The areas under the load-deflection curves in Fig. 5 characterize the energy absorption. The capability of a quasibrittle structure to absorb energy decreases, in relative terms, as the structure size increases. The size effect on energy absorption capability is important for blast loads and impact.

The progressive steepening of the postpeak curves in Fig. 5 with increasing size and the development of a snapback can be most simply described by the series coupling model, which assumes that the response of a structure may be at least approximately modeled by the series coupling of the cohesive crack or damage zone with a spring characterizing the elastic unloading of the rest of the structure (Bažant and Cedolin 1991, Sec. 13.2, Bažant 2000).

One possible exception to the behavior described above is in the fracture of fiber-reinforced concrete (FRC), where the larger crack opening that occurs in bigger specimens/structures mobilizes the fibers more effectively. This results in more ductile response after cracking in larger specimens of similar geometry as seen in Fig. 6, where experimental results (Jamet et al., 1995) from tests of two sizes of plain concrete (PC) and FRC beams are compared.

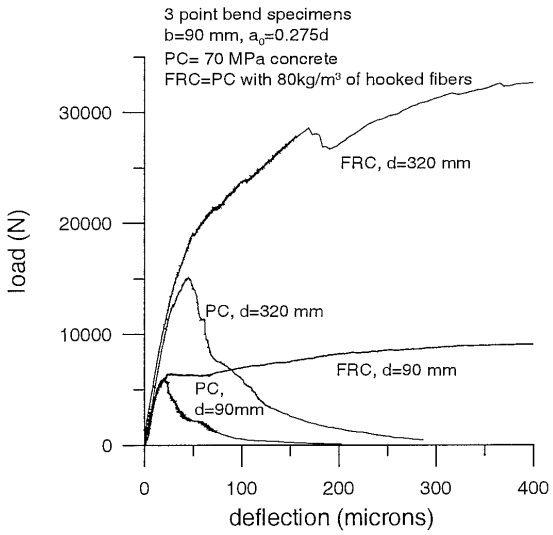

Fig. 6 – Load-deflection curves of plain concrete and fiber-reinforced concrete beams of different sizes (after Jamet et al., 1995.

6.4 Asymptotic analysis of size effect by equivalent LEFM

To obtain simple approximate size effect formulae that give a complete prediction of the failure load, including the effect of geometrical shape of the structure, equivalent LEFM may be used. In this approach the tip of the equivalent LEFM (sharp) crack is assumed to lie at distance c_f ahead of the tip of the traction-free crack or notch, c_f being a constant (representing roughly one half of the length of the

FPZ ahead of the tip. Two cases are relatively simple: (i) If a large crack grows stably prior to P_{max} or if there is a long notch,

$$\sigma_N = \frac{\sqrt{EG_f} + \sigma_Y\sqrt{\gamma'(\alpha_0)c_f + \gamma(\alpha_0)D}}{\sqrt{g'(\alpha_0)c_f + g(\alpha_0)D}} \quad (14)$$

and (ii) if P_{max} occurs at fracture initiation from a smooth surface

$$\sigma_N = \frac{\sqrt{EG_f} + \sigma_Y\sqrt{\gamma'(0)c_f + \gamma''(0)(c_f^2/2D)}}{\sqrt{g'(0)c_f + g''(0)(c_f^2/2D)}} \quad (15)$$

(Bažant 1997b, Bažant 1998) where the primes denote derivatives; $g(\alpha_0) = K_{IP}^2/\sigma_N^2 D$ and $\gamma(\alpha_0) = K_{I\sigma}^2/\sigma_Y^2 D$ are dimensionless energy release functions of LEFM of $\alpha = a_0/D$ where a_0 = length of notch or crack up to the beginning of the FPZ; K_{IP}, $K_{I\sigma}$ = stress intensity factors for load P and for loading by uniform residual crack-bridging stress σ_Y, respectively; $\sigma_Y = 0$ for tensile fracture, but $\sigma_Y \neq 0$ in the cases of compression fracture in concrete, kink band propagation in fiber composites, and tensile fracture of composites reinforced by fibers short enough to undergo frictional pullout rather than breakage. The asymptotic behavior of (14) for $D \to \infty$ is of the LEFM type, $\sigma_N - \sigma_{Y\infty} \propto D^{-1/2}$ where $\sigma_{Y\infty} = \sigma_Y\sqrt{\gamma(\alpha_0)/g(\alpha_0)}$. Formula (15) approaches for $D \to \infty$ a finite asymptotic value. So does formula (14) if $\sigma_Y > 0$. Note that parameter G_f in (14)–(15) is related to but different from the fracture energy G_F, as will be explained in the next subsection.

6.5 Size-effect method for measuring material fracture parameters and R-curve

Comparison of (14) with (11) yields the relations:

$$D_0 = c_f g'(\alpha_0)/g(\alpha_0) \quad (16)$$

$$B\sigma_0 = \sqrt{EG_f/c_f g'(\alpha_0)} \quad (17)$$

Therefore, by fitting formula (11) with $\sigma_R = 0$ to the values of σ_N measured on test specimens of different sizes with a sufficiently broad range of brittleness numbers[1]

$$\beta = \frac{D}{D_0} = \frac{g(\alpha_0)}{c_f g'(\alpha_0)} \quad (18)$$

the values of G_f and c_f can be identified (Bažant and Pfeiffer 1987, Bažant and Kazemi 1990). The fitting can be best done by using the Levenberg-Marquardt nonlinear optimization algorithm, but it can also be accomplished by a (properly weighted) linear regression of σ_N^{-2} versus D. The specimens do not have to be geometrically similar, although when they are the evaluation is simpler and the error smaller. The lower the scatter of test results, the narrower is the minimum necessary range of β (for concrete and fiber composites, the size range $1:4$ is the minimum).

The size effect method of measuring fracture characteristics has been adopted for an international standard recommendation for concrete (RILEM 1990, [BP] Sec. 6.3), and has also been verified and used for various rocks, ceramics, orthotropic fiber-polymer composites, sea ice, wood, tough metals and other quasibrittle materials. The advantage of the size effect method is that the tests, requiring only the maximum loads, are foolproof and easy to carry out.

With regard to the cohesive crack model, note that the size effect method gives the energy value corresponding to the area under the initial tangent of the softening stress-displacement curve, rather than the total area under the curve. The stress-displacement curves used by cohesive crack models for concrete typically start by a relatively steep descending part followed by a long tail. The area under the entire stress-displacement curve corresponds to the fracture energy G_F that would be consumed per unit area of the crack advance in an infinitely large specimen. Laboratory specimens used by the size-effect method are not large enough to activate the long tail of the curve already before peak, and the peak load is usually attained with only a partially developed process zone. Consequenly, the shape of the tail has no influence on the peak load and the corresponding part of the fracture energy cannot be captured by the size-effect method. This is why, for the usual range of sizes tested in the laboratory, the fracture energy G_f identified from the size effect law is smaller than the fracture energy for an infinite specimen, G_F, which can be approximately determined by the work-of-fracture method (RILEM 1985). Parameter G_f can be roughly understood as the area under the initial tangent of the softening stress-displacement curve, and the typical ratio $G_f : G_F$ is about $1 : 2.5$.

The size effect method also permits determining the R-curve (resistance curve) of the quasibrittle material—a curve that represents the apparent variation of fracture energy with crack extension for

[1] A practically useful brittleness number should be independent of structure geometry. This condition is satisfied by definition (18) proposed by Bažant (1987) on the basis of the size effect law. The term brittleness number was applied earlier to other quantities, which however lack the crucial geometry factor g'/g and thus are not generally applicable. This is the case for the so-called 'brittleness numbers' proposed by Gogotsi et al. (1978) and Homeny et al. (1980); and also for the ratio D/l_{ch} where l_{ch} is Irwin's characteristic length introduced in a discussion of brittleness by Irwin and later called the 'brittleness number' by Hillerborg (1985); and furthermore for the ratio $G_F/(\sigma_0 D)$ called the 'brittleness number' by Carpinteri (1981). With these earlier definitions, the value $\beta = 2$ could for instance mean a very brittle behavior for one geometry, and a very ductile behavior for another geometry, making the term 'brittleness number' meaningless.

which LEFM becomes approximately equivalent to the actual material with a large FPZ. The R-curve, which (in contrast to the classical R-curve definition) depends on the specimen geometry, can obtained as the envelope of the curves of the energy release rate at $P = P_{max}$ (for each size) versus the crack extension for specimens of various sizes. In general, this can easily be done numerically, and if the size effect law has the form in (11) with $\sigma_R = 0$, a parametric analytical expression for the R-curve exists (Bažant and Kazemi 1990, [BP] Sec. 6.4).

The fracture model implied by the size effect law in (11) or (14) has one independent characteristic length, c_f, representing about one half of the FPZ length. From c_f, using the relation $\ell_1 = B^2 g'(\alpha_0) c_f$, one can determine the characteristic length $\ell_1 = E' G_f / f_t'^2$ where G_f represents the area under the initial tangent of the softening stress-separation curve of the cohesive crack model and must be distinguished from fracture energy G_F, which represents the area under the entire softening curve and is measured by the work-of-fracture method (the ratio G_F/G_f exhibits very high scatter and on the average is about 2.5, which means that ℓ_0/ℓ_1 is on the average about 2.5); Bažant, Yu and Zi (2002). The value of c_f controls the size D_0 at the center of the bridging region (intersection of the power-law asymptotes in Fig. 1c, and σ_0 or G_f controls a vertical shift of the size effect curve at constant D_0. Aside from geometry factors expressed in terms of function $g(\alpha)$, the locations of the large-size and small-size asymptotes depend only on $K_c = \sqrt{EG_f}$ and EG_f/c_f, respectively.

A very effective method for measuring G_f has been the notched-unnotched method, conceived by Guinea, Planas and Elices (1994a,b) without any reference to size effect. Bažant, Yu and Zi (2002) recently improved this method by exploiting the exact dimensionless size effect curve of the cohesive crack model which is calculated in advance for given specimen geometry. This is possible because only the initial downward slope of the softening curve matters for the maximum load. The reason is that, in normal-size notched specimens, the crack stress profile at maximum load terminates at notch tip with a finite stress so large that the tail portion of the softening curve is not reached. The improved method, as well as Guinea et al.'s, makes it possible to determine G_f (or the initial slope of the softening curve) simply by measuring solely the maximum loads of notched specimens of only one size (and one geometry), supplemented by direct measurement of f_t' (for which the Brazilian split-cylinder test has been recommended). If the cohesive crack model is assumed to hold for the entire size range $D \in (0, \infty)$, then the strength data correspond to the zero-size limit of the size effect plot (i.e., to zero brittleness number, Bažant and Li 1996) because $\lim \sigma_N$ for $D \to 0$ depends only on the tensile strength (being independent of the softening curve). The Bažant-Yu-Zi method uses the regression equation

$$Y = AX + C - \Delta(X) \tag{19}$$

with

$$X = D/\ell_1, \;\; Y = (f_t'/\sigma_N)^2 \tag{20}$$

Function $\Delta(X)$, which must be accurately computed in advance, gives the deviations of the exact size effect curve of the cohesive crack model from the size effect law (11) (with $\sigma_R = 0$); $\Delta(X)$ vanishes for $D \to \infty$ and its asymptotic expansion begins with the term $1/D^2$. For normal-size notched three-point bend specimens, the correction $\Delta(X)$ is insignificant (error of a few percent only), but for zero size the correction by $\Delta(0)$ is important (Bažant, Yu and Zi 2002). Knowing function $\Delta(X)$, including the limit $\Delta(0)$, Eq. (19) can be fitted to the measured σ_N values for notched specimens of one size and the σ_N values corresponding to f_t' at zero-size limit. The fitting yields the values of A and C, from which G_f, c_f and ℓ_1 follow (Bažant, Yu and Zi 2002).

The improved size effect method of Bažant, Yu and Zi is equivalent to Guinea et al.'s method except for the statistical evaluation. The fact that the former permits identification of material parameters by statistical regression of both the notched specimen data and the strength data is an advantage.

6.6 Critical crack-tip opening displacement, δ_{CTOD}

The quasibrittle size effect, bridging plasticity and LEFM, can also be simulated by the fracture models characterized by the critical stress intensity factor K_c (fracture toughness) and δ_{CTOD}; for metals see Wells (1961) and Cottrell (1963), and for concrete Jenq and Shah (1985). Jenq and Shah's model, called the two-parameter fracture model, has been shown to give similar results as the R-curve derived from the size effect law in (11) with $\sigma_R = 0$. The approximate relationship of size effect law and Jenq-Shah model is given by

$$K_c = \sqrt{EG_f} \tag{21}$$

$$\delta_{CTOD} = \frac{1}{\pi}\sqrt{\frac{8G_f c_f}{E}} \tag{22}$$

However, Jenq-Shah model suffers from a dependence of its results on the slope of the unloading curve of the cohesive crack model (this dependence can change the measured G_f within a range of about 15% and is, in principle, inadmissible because the fracture energy is defined by the softening curve independently of the unloading properties of the cohesive crack model); Bažant, Yu and Zi (2002). Using (21) and (22), the values of K_c and δ_{CTOD} can be easily identified by fitting the size effect law (11) to measured values of the peak load P_{max}.

Like the size effect law in (11) with $\sigma_R = 0$, the two-parameter model has only one independent characteristic length, δ_{CTOD}, which is related to ℓ_1 or c_f.

6.7 Material heterogeneity and representative volume element

The smallest specimens in size effect tests have often been only about five aggregate sizes in cross section dimension. One may wonder whether this is enough in view of the concept of the representative volume element (RVE). The answer depends of statistical considerations.

The RVE is defined as the smallest element which, when translated through the heterogeneous material, does not change its statistical properties. But what statistical properties? And with what accuracy? There is much confusion in the literature stemming from ignorance of the statistical aspect.

If one considers the moments of the probability distributions of the strength and stiffness parameters up to infinite order, and demands complete accuracy, an RVE would have to be infinitely large (and continuum mechanics inapplicable at any size) unless that material has an artificial perfectly periodic structure. For the first two moments of the distribution (i.e., including the invariance of the standard deviation during RVE shifts), the RVE must be much larger than for the first moment only, i.e., for the mean response (as long as the shifting of the RVE through a single specimen is considered).

Therefore, if the test results are evaluated statistically, the RVE can in practice be quite small. This is confirmed by the fact that the mean of size effect evaluated statistically from many specimens exhibits a rather smooth extension of the trend observed for large sizes, even though continuum mechanics applied to one specimen alone, without statistical averaging, would lead to gross random scatter.

7 EXTENSIONS, RAMIFICATIONS AND APPLICATIONS

7.1 Size effects in compression fracture

Loading by high compressive stress without sufficient lateral confining stresses leads to damage in the form of axial splitting microcracks engendered by pores, inclusions or inclined slip planes. This damage localizes into a band that propagates either axially or laterally.

For axial propagation, the energy release from the band drives the formation of the axial splitting fracture, and since this energy release is proportional to the length of the band, there is no size effect. For lateral propagation, the stress in the zones on the sides of the damage band gets reduced, which causes an energy release that grows in proportion to D^2, while the energy consumed and dissipated in the band grows in proportion to D. The mismatch of energy release rates inevitably engenders a deterministic size effect of the quasibrittle type, analogous to the size effect associated with tensile fracture. In consequence of the size effect, failure by lateral propagation must prevail over the failure by axial propagation if a certain critical size is exceeded.

The size effect can again be approximately described by the equivalent LEFM. This leads to Eq. (14) in which σ_Y is determined by analysis of the microbuckling in the laterally propagating band of axial splitting cracks. The spacing s of these cracks is in (14) assumed to be dictated by material inhomogeneities. However, if the spacing is not dictated and is such that it minimizes σ_N, then the size effect gets modified as:

$$\sigma_N = CD^{-2/5} + \sigma_\infty \tag{23}$$

([BP] Sec. 10.5.11) where C, σ_∞ = constants, the approximate values of which have been calculated for the breakout of boreholes in rock.

7.2 Fracturing truss model for concrete and boreholes in rock

Propagation of compression fracture is what appears to control the maximum load in diagonal shear failure of reinforced concrete beams with or without stirrups, for which a very strong size effect has been demonstrated experimentally (e.g. Walraven 1995, Walraven and Lehwalter 1994, Bažant and Kazemi 1991, Kani 1967, Iguro et al. 1985, Bažant 1997a, Okamura and Maekawa 1994, Reinhardt 1981, Shioya and Akiyama 1994). A long diagonal tension crack grows stably under shear loading until the concrete near its tip gets crushed. A simplified formula for the size effect can be obtained by energetic modification of the classical truss model (strut-and-tie model) (Bažant 1997a).

The explosive breakout of boreholes (or mining stopes) in rock under very high pressures is know to also exhibit size effect, as revealed by the tests of Carter (1992), Carter et al. (1992), Haimson and Herrick (1989) and Nesetova and Lajtai (1973). An approximate analytical solution can be obtained by exploiting Eschelby's theorem for eigenstresses in elliptical inclusions (Bažant et al. 1993).

7.3 Kink bands in fiber composites

A kink band, in which axial shear-splitting cracks develop between fibers which undergo microbuckling, is one typical mode of compression failure of composites or laminates with uniaxial fiber reinforcement. This failure mode, whose theory was

begun by Rosen (1965) and Argon (1972), was until recently treated by the theory of plasticity, which implies no size effect. Recent experimental and theoretical studies (see Budianski et al. 1997), however, revealed that the kink band propagates side-way like a crack and the stress on the flanks of the band gets reduced to a certain residual value, which is here denoted as σ_Y and can be estimated by the classical plasticity approach of Budianski (1983). The crack-like behavior implies a size effect, which is demonstrated by the latest Bažant et al. 's (1999) laboratory tests of notched carbon-PEEK specimens (Fig. 4); these tests also demonstrated the possibility of a stable growth of a long kink band, which was achieved by rotational restraint at the ends).

There are again two types of size effect, depending on whether P_{max} is reached (i) when the FPZ of the kink band is attached to a smooth surface or (ii) or when there exists either a notch or a long segment of kink band in which the stress has been reduced to σ_Y. Formulae (14) and (15), respectively, approximately describe the size effects for these two basic cases; in this case G_f now plays the role of fracture energy of the kink band (area below the stress-contraction curve of the kink band and above the σ_Y value), and c_f the role of the FPZ size of the kink band, which is assumed to be approximately constant, governed by material properties.

The aforementioned carbon-PEEK tests also confirm that case (ii), in which a long kink band grows stably prior to P_{max}, is possible (in those test, this is by virtue of a lateral shift of compression resultant in wide notched prismatic specimens with ends restrained against rotation).

7.4 Size effects in sea ice and snow

Normal laboratory specimens of sea ice exhibit no notch sensitivity. Therefore, failure of sea ice has been thought to be well described by plastic limit analysis, which exhibits no size effect (e.g. Sodhi 1995, Kerr 1996). This perception, however, changed drastically after Dempsey carried out in 1993 on the Arctic Ocean size effect tests of floating notched square specimens with an unprecedented, record-breaking size range (with square sides ranging from 0.5 m to 80 m!) (see Dempsey et al. 1995a, 1999, Mulmule et al. 1995).

It is now clear that floating sea ice plates are quasibrittle and their size effect on the scale of 100 m approaches that of LEFM. Among other things, Dempsey's major experimental result explains why the measured forces exerted by moving ice on a fixed oil platform are one to two orders of magnitude smaller than the predictions of plastic limit analysis based on the laboratory strength of ice. The size effect law in (11) with σ_R = 0, or in (14) (with σ_Y = 0), agrees with these results well, permitting the values of G_f and c_f of sea ice to be extracted by linear regression of the P_{max} data. The value of c_f is in the order of meters (which can be explained by inhomogeneities such as brine pockets and channels, as well as preexisting thermal cracks, bottom roughness of the plate, warm and cold spots due to alternating snow drifts, etc.). Information on the size effect in sea ice can also be extractic from acoustic measurements (Li and Bažant, 1998).

Rapid cooling in the Arctic can produce in the floating plate bending moments large enough to cause fracture. According to plasticity or elasticity with a strength limit, the critical temperature difference ΔT_{cr} across the plate would have be independent of plate thickness D. Fracture analysis, however, indicated a quasibrittle size effect. Curiously, its asymptotic form is not $\Delta T_{cr} \propto D^{-1/2}$ but

$$\Delta T_{cr} \;\propto\; D^{-3/8} \tag{24}$$

(Bažant 1992). The reason is that D is not a characteristic dimension in the plane of the boundary value problem of plate bending; rather it is the flexural wavelength of a plate on elastic foundation, which is proportional to $D^{3/4}$ rather than D. It seems that (24) may explain why long cracks of length 10 to 100 km, which suddenly form in the fall in the Arctic ice cover, often run through thick ice floes and do not follow the thinly refrozen water leads around the floes.

In analyzing the vertical penetration of floating ice plate (load capacity for heavy objects on ice, or the maximum force P required for penetration from below), one must take into account that bending cracks are reach only through part of the thickness, their ligaments transmitting compressive forces, which produces a dome effect. Because at maximum load that part-through bending crack (of variable depth profile) is growing vertically, the asymptotic size effect is not $P/D^2 = \sigma_N \propto D^{-3/8}$ (Slepyan 1990) but $\sigma_N \propto D^{-1/2}$. This was determined by a simplified analytical solution (with a uniform crack depth) by Dempsey et al. (1995b), and confirmed by a detailed numerical solution with a variable crack depth profile (Bažant and Kim 1998). The latter also led, to an approximate prediction formula for the entire practical range of D, which is of the type of (11) with σ_N = 0. This formula was shown to agree with the existing field test (Frankenstein 1963, 1966; Lichtenberger et al. 1974).

Analytical solutions of size effect in sea ice were presented by Bažant (2002b) and Bažant and Guo (2002). Recent analysis (Bažant, Zi and McClung 2003) also revealed a significant size effect in the triggering of dry slab snow avalanches.

7.5 Influence of crack separation rate, creep and viscosity

There are two mechanisms in which the loading rate affects fracture growth: (i) creep of the material outside the FPZ, and (ii) rate dependence of the severance of material bonds in the FPZ. The latter may be modeled as a rate process controlled by activation energy, with Arrhenius type temperature dependence. This leads to a dependence of the softening stress-separation relation of the cohesive crack model on the rate of opening displacement. In an equivalent LEFM approach, the latter is modeled by considering the crack extension rate to be a power function of the ratio of the stress intensity factor to its critical R-curve value.

For quasibrittle materials exhibiting creep (e.g. concretes and polymer composites, but not rocks or ceramics), the consequence of mechanism 1 (creep) is that a decrease of loading rate, or an increase of duration of a sustained load, causes a decrease of the effective length of the FPZ. This in turn means an increase of the brittleness number manifested by a leftward shift of the size effect curve in the plot of $\log \sigma_N$ versus $\log D$, i.e. a decrease of effective D_0. For slow or long-time loading, quasibrittle structures become more brittle and exhibit a stronger size effect (Bažant and Li 1997).

Mechanism 2 (rate dependence of separation) causes that an increase of loading rate, or a decrease of sustained load duration, leads to an upward shift of the size effect curve for $\log \sigma_N$ but has no effect on D_0 and thus on brittleness (this mechanism also explains an interesting recently discovered phenomenon—a reversal of softening to hardening after a sudden increase of the loading rate, which cannot be explained by creep).

So far all our discussions dealt with statics. In dynamic problems, any type of viscosity η of the material (present in models for creep, viscoelasticity or viscoplasticity) implies a characteristic length. Indeed, since η has the dimension of stress over strain rate, i.e., kg / m s, and the Young's modulus E and mass density ρ have dimensions $[E] =$ kg / m s^2 and $[\rho] =$ kg / m^3, the material length associated with viscosity is given by

$$\ell_v = \frac{\eta}{v\rho}, \qquad v = \sqrt{\frac{E}{\rho}} \tag{25}$$

where v = longitudinal wave speed. Consequently, any rate dependence in the constitutive law implies a size effect. There is, however, an important difference. Unlike the size effect associated with ℓ_0 or c_f, the viscosity-induced size effect (as well as the width of damage localization zones) is not time independent. It varies with the rates of loading and deformation of the structure and vanishes as the rates drop to zero. For this reason, an artificial viscosity or rate effect can approximate the nonviscous size effect and localization only within a narrow range of time delays and rates, but not generally.

7.6 Environmental influences on size effect

Drying and temperature changes are known to produce very large stresses and damage in concrete. So it is natural to expect that they could modify the size effect curves considerably.

Drying of concrete produces large self-equilibrated stresses in the cross sections of concrete structures. These stresses lead to microcracking as well as continuous cracks, and can have a major effect on the deformation under superimposed applied loads. But this effect has a tremendous variability. In large structures, where the size effect is of most interest, drying is a very slow process. The depth of penetration of a drying front into a wall is roughly proportional to $\sqrt{t}$ where t is the drying time. The drying half-time is about one year for a 15 cm slab and increases in proportion to the square of thickness, which means that it is about 40 years for a 1 m thick wall. The time to closely approach moisture equilibrium is about 20 years for a 15 cm slab and 800 years for a 1 m thick wall. These times and moisture content distributions strongly depend on the cross section shape. For thick structures drying very slowly, creep causes a major relaxation of the internal stresses, but has relatively little effect in small test specimens (which therefore show greater effects of drying). Consequently, the alteration of size effect in large drying structures must generally be expected to be much smaller than in laboratory specimens. At the beginning of drying, the surface layer of load-free specimens is in tension and undergoes microcracking, but in a late stage of drying the surface layer goes into compression while the core is subjected to tension, which is explained by creep and the irreversibilty of crack opening. Cyclic environment affects only the surface layer of thick structures. Temperature changes have similar effects and, especially when simultaneous with drying, further complicate the behavior.

Thanks to development of realistic models for drying and thermal effects in concrete and finite element computational approaches (Roelfstra, Sadouki and Wittmann, 1985; Bažant and Chern, 1985; Bažant and Xi, 1994; Coussy, 1995; Lewis and Schrefler, 1998; Hellmich, Ulm and Mang, 1999; Torrenti et al., 1999; Sadouki and Wittmann, 2001; Acker 2001; Bažant, Cusatis and Cedolin, 2003), the effects of drying and wetting can nowadays be simulated numerically quite well. Coupling the drying and thermal effects with the computational models for tensile and compressive fracturing and failure analysis (e.g., in the manner of Bažant and Xi 1994), the designers of sensitive special structures have today the means for calculating the failure loads of

structures subjected to drying and thermal effects. In this way, using state-of-art material models and having adequate information on the hygrothermal material properties, one can realistically predict the modification of size effect under these influences. For instance, Planas and Elices (1992, 1993) evaluated numerically the size effect on the modulus of rupture and showed that it strongly depends on the shrinkage strains induced by drying.

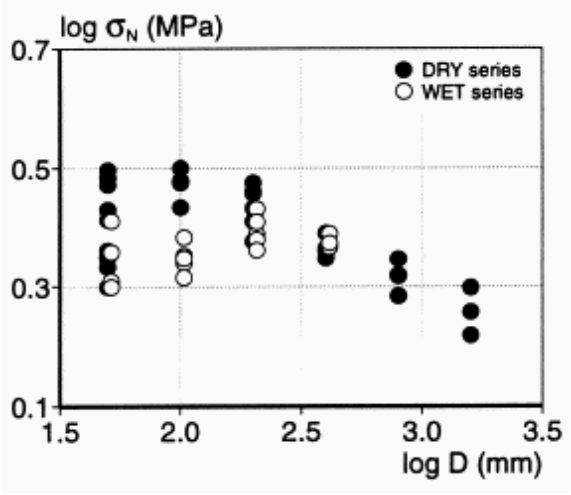

Fig. 7 – Effect of drying conditions on nominal tensile strength of concrete (after van Vliet and van Mier, 2000).

The fact that the influence of drying can be large is documented by recent excellent tests of van Vliet and van Mier (1999, 2000) in Delft, the results of which are reproduced in Fig. 7. As one can see, drying can even reverse the size effect in small test cylinders subjected to drying for a certain period of time. However, very different results must be expected for specimens tested to failure at different times of the drying process, for different specimen sizes and shapes, different environmental humidities and histories.

In view of the great number of factors governing these environmental effects, searching for a simple formula that takes the environmental influences into account is doubtless futile. Detailed predictions will always depend on computer simulations. But one observation is pertinent: The size effect in very large structures will usually be affected by drying much less than small laboratory specimens since their cores do not suffer drying for the entire lifetime. In these cases of main interest, the simple size effect laws calibrated on specimens that have not suffered drying may be expected to give reasonable predictions .

7.7 Size effect in fatigue crack growth

Cracks slowly grow under fatigue (repeated) loading. This is for metals and ceramics described the Paris (or Paris-Erdogan) law, which states that plot of the logarithm of the crack length increment per cycle versus the amplitude of the stress intensity factor in logarithmic scale is a rising straight line. For quasibrittle material it turns out that a size increase causes this straight line to shift to the right, the shift being derivable from the size effect law in (11) ([BP] Sec. 11.7).

7.8 Size effect for cohesive crack model and crack band model

The cohesive crack model (called by Hillerborg et al., 1976, and Petersson, 1981, the fictitious crack model) is more accurate yet less simple than the equivalent LEFM. It is based of the hypothesis that there exists a unique decreasing function $w = g_w(\sigma)$ relating the crack opening displacement w (separation of crack faces) to the crack bridging stress σ in the FPZ. The obvious way to determine the size effect is to solve P_{max} by numerical integration for step-by-step loading (Petersson 1981).

The size effect plot, however, can be solved directly if one inverts the problem, searching the size D for which a given relative crack length $\alpha = a/D$ corresponds to $P_{\max}$. This leads to the equations (Li and Bažant 1996):

$$D \int_{\alpha_0}^{\alpha} C^{\sigma\sigma}(\xi,\xi')\, v(\xi')\, d\xi' = -\, g'_w[\sigma(\xi)]\, v(\xi) \tag{26}$$

$$P_{\max} = \frac{\int_{\alpha_0}^{\alpha} v(\xi)\, d\xi}{D \int_{\alpha_0}^{\alpha} C^{\sigma P}(\xi)\, v(\xi)\, d\xi} \tag{27}$$

where the first represents an eigenvalue problem for a homogeneous Fredholm integral equation, with D as the eigenvalue and $v(\xi)$ as the eigenfunction; $\xi = x/D$, x = coordinate along the crack (Fig. 8); $\alpha = a/D$, $\alpha_0 = a_0/D$; a, a_0 = total crack length and traction-free crack length (or notch length); $C^{\sigma\sigma}(\xi,\xi')$, $C^{\sigma P}(\xi)$ = compliance functions of structure for crack surface force and given load P; $v(\xi)$ has the meaning of the derivative $\mathrm{d}\sigma(\xi)/\mathrm{d}\xi$; $g'_w = \mathrm{d}g_w/\mathrm{d}\sigma$ is the inverse slope of the stress-separation curve. When this slope is considered constant (which is the case of linear softening, sufficient for most applications), the eigenvalue problem is linear, but when the slope is considered variable, the eigenvalue problem is nonlinear, in which case it may be solved iteratively. In the first iteration, the g'_w values at all crack points are assumed to be equal to the initial slope of the stress separation curve, which makes the eigenvalue problem in (26) linear and directly solvable. After calculating new D and P_{max}, one must obtain σ for each crack point, from which one can evaluate new slope g'_w for each point. All g'_w values being fixed, the new eigenvalue problem in (26) is again linear and the procedure may be iterated. For detailed explanation, see Zi and Bažant (2003) who also give generalization for a softening law terminating with a finite residual stress (used for

simulating kink bands in fiber composites, Bažant et al. 1999).

These results have also been extended to obtain directly the load and displacement corresponding, on the load-deflection curve, to a point with any given tangential stiffness, including the displacement at the snapback point which characterizes the ductility of the structure.

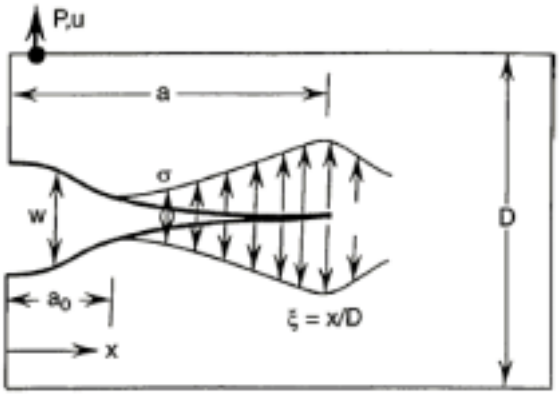

Fig. 8 – Cohesive crack and distribution of crack-bridging stresses.

The cohesive crack model possesses at least one, but for concrete typically two, independent characteristic lengths: $\ell_0 = EG_F/\sigma_0^2$ and $\ell_1 = EG_f/\sigma_0^2$ where G_F = area under the entire softening stress-displacement curve $\sigma = f(w)$, and G_f = area under the initial tangent to this curve, which is equal to G_F only if the curve is simplified as linear (typically $G_F \approx 2.5G_f$). The bilinear stress-displacement law used for concrete involves further parameters of the length dimension—the opening displacement w_f when the stress is reduced to zero at the displacement at the change of slope, but their values are implied by G_f, G_F, σ_0 and the stress at the change of slope.

The scatter of size effect measurements within a practicable size range (up to 1:30) normally does not permit identifying more than one characteristic length (measurements of postpeak behavior are used for that purpose). Vice versa, when only the maximum loads of structures in the bridging region between plasticity and LEFM are of interest, hardly more than one characteristic length (namely c_f) is needed.

The crack band model, which is easier to implement is used in commercial codes (e.g. DIANA, SBETA; Červenka and Pukl 1994), is for localized cracking or fracture, nearly equivalent to the cohesive crack model ([BP], Planas et al. 1993), provided that the effective (average) transverse inelastic strain in the crack band is taken as $\epsilon_y = w/h$ where h is the width of the band. All that has been said about the cohesive crack model also applies to the crack band model. Width h, of course, represents an additional characteristic length, $\ell_4 = h$, It matters only when the cracking is not localized but distributed (e.g. due to the effect of dense and strong enough reinforcement), and it governs the spacings of parallel cracks. Their spacing cannot be unambiguously captured by the cohesive crack model.

7.9 Size effect via nonlocal, gradient or discrete element models

The hypostatic feature of any model capable of bridging the power law size effects of plasticity and LEFM is the presence of some characteristic length, ℓ. In the equivalent LEFM associated with the size effect law in (11), c_f serves as a characteristic length of the material, although this length can equivalently be identified with δ_{CTOD} in Wells-Cottrell or Jenq-Shah models, or with the crack opening w_f at which the stress in the cohesive crack model (or crack band model) is reduced to zero (for size effect analysis with the cohesive crack model, see [BP] and Bažant and Li 1995).

In the integral-type nonlocal continuum damage models, ℓ represents the effective size of the representative volume of the material, which in turn plays the role of the effective size of the averaging domain in nonlocal material models. In the second-gradient nonlocal damage models, which may be derived as an approximation of the integral-type nonlocal damage models, a material length is involved in a relation combining the strain with its Laplacian. In damage simulation by the discrete element (or random particle) models, the material length is represented by the statistical average of particle size.

The existence of ℓ in these models engenders a quasibrittle size effect that bridges the power-law size effects of plasticity and LEFM and follows closely equation (11) with σ_N = 0, as documented by numerous finite element simulations. It also poses a lower bound on the energy dissipation during failure, prevents spurious excessive localization of softening continuum damage, and eliminates spurious mesh sensitivity ([BP], ch. 13).

These important subjects will not be discussed here any further because there exist recent extensive reviews (Bažant 1999, Bažant and Jirásek 2002).

7.10 Nonlocal statistical generalization of Weibull theory

Two cases need to be distinguished: (a) The front of the fracture that causes failure can be at only one place in the structure, or (b) the front can lie, with different probabilities, at many different places. The former case occurs when a long crack whose path is dictated by fracture mechanics grows before the maximum load, or if a notch is cut in a test specimen. The latter case occurs when the maximum load is achieved at the initiation of fracture growth.

In both cases, the existence of a large FPZ calls for a modification of Weibull concept: The failure probability P_1 at a given point of the continuous structure depends not on the local stress at that point, but on the nonlocal strain, which is calculated as the average of the local strains within the neighborhood of the point constituting the representative volume of the material. The nonlocal approach broadens the applicability of Weibull concept to the case notches or long cracks, for which the existence of crack-tip singularity causes the classical Weibull probability integral to diverge at realistic m-values (in cleavage fracture of metals, the problem of crack singularity has been circumvented differently—by dividing the crack-tip plastic zone into small elements and superposing their Weibull contributions; Lei et al. 1998).

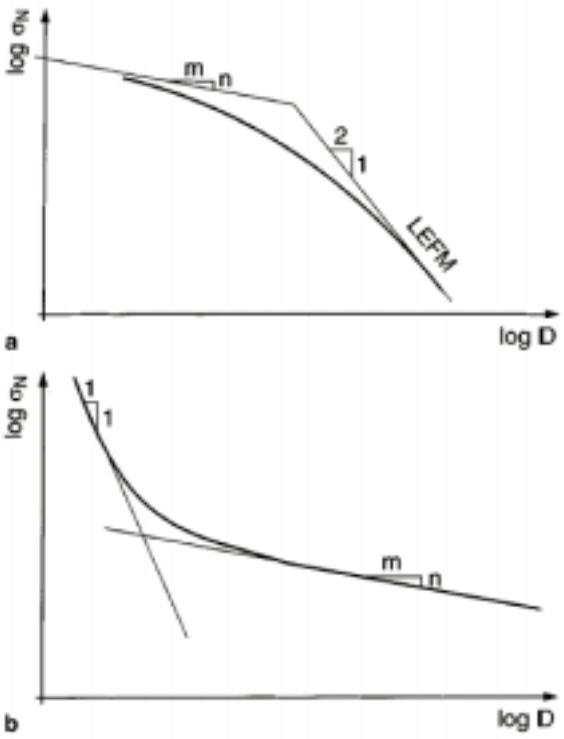

Fig. 9 – Scaling laws according to nonlocal generalization of Weibull theory for failures after long stable crack growth (a) or at crack initiation (b).

Using the nonlocal Weibull theory (Bažant and Xi 1991, Bažant and Novák 2000a, 2000b, 2000c), one can show that the proper statistical generalizations of (11) (with $\sigma_R = 0$) and (13) having the correct asymptotic forms for $D \to \infty$, $D \to 0$ and $m \to \infty$ are (Fig. 9):

Case (a):

$$\sigma_N = B\sigma_0 \left(\beta^{2rn_d/m} + \beta^r\right)^{-1/2r} \quad (28)$$

$$\beta = D/D_0 \quad (29)$$

Case (b):

$$\sigma_N = \sigma_0 \zeta^{n_d/m} \left(1 + r\zeta^{1-rn_d/m}\right)^{1/r} \quad (30)$$

$$\zeta = D_b/D \quad (31)$$

where it is assumed that $rn_d < m$, which is normally the case.

The first formula, which was obtained for $r = 1$ by Bažant and Xi (1991) and refined for $n \neq 1$ by Planas, has the property that the statistical influence on the size effect disappears asymptotically for large D. The reason is that, for long cracks or notches with stress singularity, a significant contribution to the Weibull probability integral comes only from the FPZ, whose size does not vary much with D. The second formula has the property that the statistical influence asymptotically disappears for small sizes. The reason is that the FPZ occupies much of the structure volume.

Numerical analyses of test data for concrete show that the size ranges in which the statistical influence on the size effect in case (a) as well as (b) would be significant do not lie within the range of practical interest. Thus, the deterministic size effect dominates and its statistical correction in (28) and (30) may be ignored for concrete, except in the rare situations where the deterministic size effect vanishes, which occurs rarely (e.g., for centric tension of an unreinforced bar).

7.11 Other types of size effect

Aside from the statistical and quasibrittle size effects, there are further types of size effect that influence nominal strength:

1. The boundary layer effect, which is due to material heterogeneity (i.e., the fact that the surface layer of heterogeneous material such as concrete has a different composition because the aggregates cannot protrude through the surface), and to Poisson effect (i.e., the fact that a plane strain state on planes parallel to the surface can exist in the core of the test specimen but not at its surface).

2. The existence of a three-dimensional stress singularity at the intersection of crack edge with a surface, which is also caused by the Poisson effect ([BP], Sec. 1.3). This causes the portion of the FPZ near the surface to behave differently from that in the interior.

Size effect is also observed in delamination fracture that occurs in the interface between concrete and fiber-reinforced plastic (FRP) laminates used in the repair and strengthening of concrete structures. When FRP laminates are subjected to tension (as in Fig. 10), the interface can fail under shear due to Mode II fracture. Considering tests on different widths of FRP laminates with unidirectional

0.117 mm thick carbon fibers bonded over a length $L_b = 100$ mm and with an (unbonded) interfacial defect of length $L_u = 40$ mm, the failure load per unit width decreases with increase in the width, as seen in the plot. This Weibull-type size effect determines the minimum width of the laminate that can be used in the laboratory characterization for obtaining the design strength (dos Santos et al., 2001).

[t]

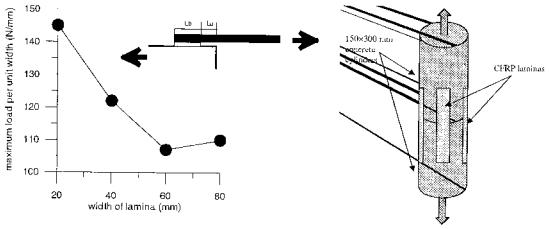

Fig. 10 – Size effect in interfacial fracture (after dos Santos et al., 2001).

An important size effect is exhibited by failure of concrete columns (Bažant and Kwon 1994, Brocca and Bazant 2002, Bažant 2002a, Burtscher 2002).

8 FRACTAL EXPLANATION OF SIZE EFFECTS

Mechanical quantities are normally referred to Euclidean geometrical entities and have integer physical dimensions. For instance, the stress is obtained as the internal force intensity per unit area and has the dimension of Nm^{-2}. For fractured or porous media, this nominal stress may not reflect the actual internal forces acting in the material microstructure. In damage mechanics, it is common to define the effective stress as the internal force intensity per unit undamaged area. Traditionally, the area that can still transmit stress is understood in the sense of Euclidean geometry.

Recently it has been suggested to model a porous fracturing material as a fractal object with a self-similar or self-affine microstructure (Goldshtein and Mosolov 1992, Mosolov and Borodich 1992, Carpinteri 1994a). If this point of view is accepted, the effective area in the traditional sense depends on the scale of observation and its Euclidean measure tends to zero as the scale is refined. Consequently, the effective stress becomes scale-dependent as well. The same holds for other mechanical quantities such as the mass density or the internal energy density (per unit volume of the bulk material, with the exclusion of pores).

The fact that the crack surfaces and microcrack distributions can be described within a certain range of scales as fractals is generally accepted. However, regarding the fractal size effect, there is no consensus yet. There are two schools of thought regarding the explanation of size effect by means of the fractality of crack surface or microcrack distributions — one positive, one skeptical.

Carpinteri (1994a) explored the possibility of handling mechanical quantities in fractal bodies by means of renormalization group transformations. The purpose was to extract macroscopic models from microscopic phenomena and to obtain the universal, i.e. scale-invariant, properties. In the fractal theory, the scale-independent mechanical quantities have noninteger physical dimensions. Energy dissipation during the fracture process is supposed to occur in an invasive fractal domain which is intermediate between a surface (LEFM hypothesis) and a volume (plasticity hypothesis). At the same time, the strength is defined with respect to a lacunar fractal domain with fractal dimension lower than 2.

A possible role of fractality in size effects of sea ice was discussed by Bhat (1990). The fractal nature of crack surfaces and of the distribution of pores and microcracks in concrete and other quasibrittle materials has been advanced as the physical origin of the size effects observed in concrete structures (Carpinteri 1994ab, Carpinteri, Chiaia and Ferro 1994, Carpinteri and Chiaia 1995). Results of uniaxial tensile tests on dog-bone shaped specimens (van Vliet and van Mier 1999, 2000, Carpinteri and Ferro 1993) suggest that the parameters characterizing the cohesive law (tensile strength, critical crack opening and fracture energy) are size-dependent, which is not taken into account by the original Hillerborg model. The assumption that energy dissipation occurs in a fractal band suggests a power-type scaling of the parameters of the cohesive law. However, this simple scaling cannot be valid on the large scale, because the self-similarity of the microstructure has an upper bound given by the size of the largest material heterogeneities. The order-disorder transition is interpreted in the form of the so-called Multifractal Scaling Laws (MFSL). For fracture energy (Carpinteri and Chiaia 1996) and tensile strength (Carpinteri, Chiaia and Ferro 1995), such laws have been proposed in the form

$$G_F(b) = G_F^{\infty}\left(1+\frac{l_{mf}}{b}\right)^{-1/2} \qquad (32)$$

$$\sigma_u(b) = f_t\left(1+\frac{l_{mf}}{b}\right)^{1/2} \qquad (33)$$

where G_F is the fracture energy, σ_u is the tensile strength, G_F^{∞} and f_t are the asymptotic values of G_F and σ_u attained in the limit of an infinite size, l_{mf} is an internal length of the material, and b is the scale of observation. These scaling laws are shown in Fig. 11.

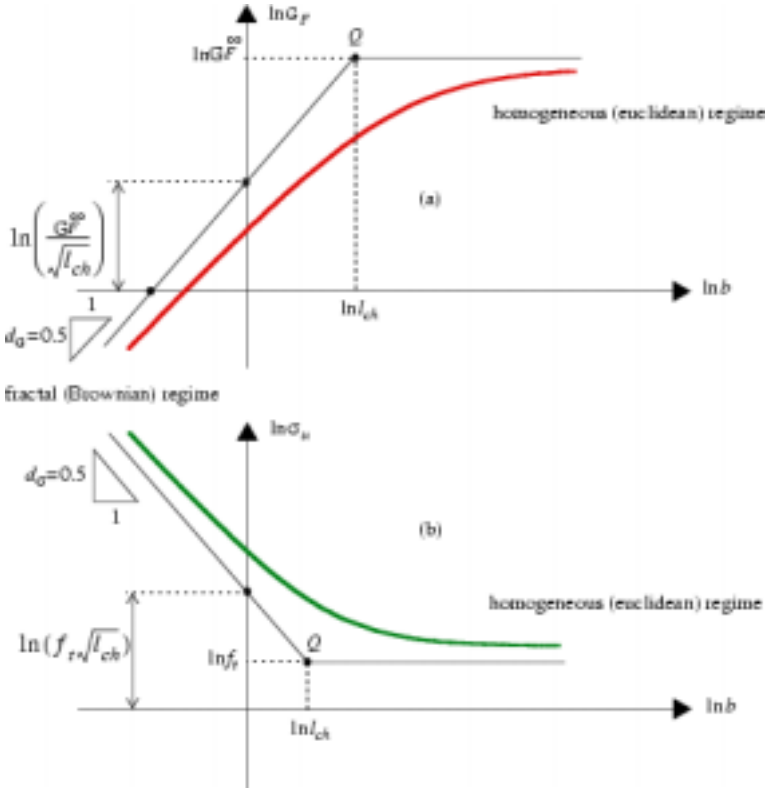

Fig. 11 – Multifractal Scaling Laws for fracture energy and tensile strength.

The dimensionless term in the parentheses, which is controlled by the ratio between the characteristic material length scale and the scale of observation, reflects the influence of disorder on the mechanical quantity measured at scale b. The transition from the fractal regime to the Euclidean one takes place around point Q at which $b = l_{mf}$. The internal length l_{mf} should be related to some characteristic size of the microstructure, for example, in the case of concrete, to the maximum aggregate size, d_{max}. The internal length parameter becomes important when the scaling behavior of two different materials is compared. For instance, in the case of a finer grained mixture, the MFSL should be shifted to the left with respect to the case of ordinary concrete, due to the lower value of l_{mf}.

Interestingly, Bažant (1998) demonstrated that eq. (33) can be obtained as a special case of formula (13), which follows from fracture mechanics, with $r = 2$. His derivation is based on considering, in the asymptotic power expansion, both the second and the third term, since the first term is practically zero in the absence of a macroscopic notch. Instead, when large stable crack growth occurs before failure, or when a macroscopic notch scaled proportionally to the size of the structure is present, energy release becomes predominant and the first term in the power expansion prevails, yielding Bažant's SEL formula (11) with $\sigma_R = 0$. The fracture explanation of eq. (33) has the advantage that the dependence of the parameters f_t and l_{mf} on the geometry can be evaluated. After a wide investigation of the existing experimental data, Carpinteri, Chiaia and Ferro (1997, 1998) concluded that the MFSL for strength (eq. 33) approximates well the behavior of unnotched structures (e.g. predicts their asymptotic finite strength), whereas formula (11) with $\sigma_R = 0$ applies to structures with large notches or with large stable crack growth prior to collapse.

The MFSL for fracture energy has been applied to many experimental results, and seems to agree very well with these data. Trends similar to those predicted by (32) can also be captured by other theories, for instance, by the theory of the local fracture energy influenced by boundary effects (Wittmann 2001). The invasive domain of energy dissipation might not be restricted to the surface, but might also be able to spread into a network of microcracks (Carpinteri, Chiaia and Nemati 1997). Moreover, fractality of the final fracture surface was used to explain R-curve behavior in quasi-brittle materials (Carpinteri and Chiaia 1996).

Bažant, Gettu, Jirásek, Planas and Xi are skeptical about the foregoing arguments and formulations. They raise the following criticisms: 1) Fractality could come only as a generalization, but not a replacement, of the energetic and statistical size effects of large cracks and large FPZ, which are undeniable. 2) The fractal concept would be of little

use as it does not provide the structure geometry dependence of size effect coefficients. 3) The argument for MFSL implies a series of hypotheses but no mathematical derivations from them. 4) The dimensional analysis argument for fractal size effect is inconclusive and inconsistent, although the renormalization group has been invoked. 5) The exponent of (33), taken as $n = 1/2$ but not proven, cannot be independent of the fractal dimension δ of cracking morphology; e.g., if $\delta \to \delta_E$ (Euclidean dimension), does $n = 1/2$ still apply even though n must be 0 for $\delta = \delta_E$? 6) Fractal explanations of the R-curve and size effect on G_F are questionable. 7) By fractality, a N-fold width increase of beams would have to cause the same size effect as a N-fold depth increase, but does not. 8) Fractality is observed for up to 1.5 orders of magnitude of refinement, which is much less than the range important for size effect laws. 9) The renormalization group transformation is insufficient since it merely gives the intersection of two power laws for adjacent scales, but not the transition which spreads over many orders of magnitude. 10) The lacunarity concept as used is at variance with the definition in mathematics (Mandelbrot, 1983). 11) Although MFSL can fit the existing modulus of rupture tests, the energetic size effect law for failure at fracture initiation fits them at least as closely.

9 CLOSING REMARKS

Substantial though the recent progress has been, the understanding of the scaling problems of solid mechanics is nevertheless far from complete. Mastering the size effect that bridges different behaviors on adjacent scales in the microstructure of material will be contingent upon the development of realistic material models that possess a material length (or characteristic length). The theory of nonlocal continuum damage will have to move beyond the present phenomenological approach based on isotropic spatial averaging, and take into account the directional and tensorial interactions between the effects causing nonlocality. A statistical description of such interactions will have to be developed. Discrete element models of the microstructure of fracturing or damaging materials will be needed to shed more light on the mechanics of what is actually happening inside the material and separate the important processes from the unimportant ones.

REFERENCES

Acker P. (2001). "Micromechanical analysis of creep and shrinkage mechanisms", in *Creep, Shrinkage and Durability Mechanics of Concrete and Other Quasi-brittle Materials*, Elsevier, Amsterdam, 15–26.

Argon, A.S. (1972). "Fracture of composites." *Treatise of Materials Science and Technology*, Vol. 1, p. 79, Academic Press, New York.

Barenblatt, G.I. (1959). "The formation of equilibrium cracks during brittle fracture. General ideas and hypothesis, axially symmetric cracks." *Prikl. Mat. Mekh.* **23** (3), 434–444.

Barenblatt, G.I. (1962). "The mathematical theory of equilibrium cracks in brittle fracture", *Advanced Appl. Mech.* **7**, 55–129.

Bažant, Z.P. (1976). "Instability, ductility, and size effect in strain-softening concrete." *J. Engng. Mech. Div., Am. Soc. Civil Engrs.*, **102**, EM2, 331–344; disc. 103, 357–358, 775–777, 104, 501–502.

Bažant, Z.P. (1984). "Size effect in blunt fracture: Concrete, rock, metal. " *J. of Engng. Mechanics*, ASCE, **110**, 518–535."

Bažant, Z.P. (1987). "Fracture energy of heterogeneous material and similitude." Preprints, SEM-RILEM *Int. Conf. on Fracture of Concrete and Rock* (held in Houston, Texas, June 1987), ed. by S.P. Shah and S.E. Swartz, publ. by SEM (Soc. for Exper. Mech.) 390–402.

Bažant, Z.P., Editor (1992). *Fracture Mechanics of Concrete Structures*, Proc., First Intern. Conf. (FraMCoS-1), held in Breckenridge, Colorado, June 1–5, Elsevier, London (1040 pp.).

Bažant, Z.P. (1992). "Large-scale thermal bending fracture of sea ice plates." *J. of Geophysical Research*, **97** (C11), 17,739–17,751.

Bažant, Z.P. (1993). "Scaling Laws in Mechanics of Failure." *J. of Engrg. Mech., ASCE*, **119** (9), 1828–1844.

Bažant, Z.P. (1997a). "Fracturing truss model: Size effect in shear failure of reinforced concrete." *J. of Engrg. Mechanics ASCE* 123 (12), 1276–1288.

Bažant, Z.P. (1997b). "Scaling of quasibrittle fracture: Asymptotic analysis." *Int. J. of Fracture* 83 (1), 19–40.

Bažant, Z.P. (1997c). "Scaling of quasibrittle fracture: Hypotheses of invasive and lacunar fractality, their critique and Weibull connection." *Int. J. of Fracture* 83 (1), 41–65.

Bažant, Z.P. (1998). "Size effect in tensile and compression fracture of concrete structures: computational modeling and design", in *Fracture Mechanics of Concrete Structures*, Proc., 3rd Int. Conf., FraMCoS-3, H. Mihashi and K. Rokugo, eds., Aedificatio Publishers, Freiburg, Germany, 1905–1922.

Bažant, Z.P. (1999). "Structural stability." *International Journal of Solids and Structures* 37, 55–67

Bažant, Z.P. (2000). "Stability of elastic, anelastic and disintegrating structures: a conspectus of main results." *Applied Mathematics and Mechanics (Zeitschrift für Angewandte Mathematik und Mechanik—ZAMM)* 80 (11/12), 709–732 (Ludwig Prandtl's 125th anniversary issue).

Bažant, Z.P. (2002a). *Scaling of Structural Strength*, Hermes Penton Science, London.

Bažant, Z.P. (2002b). "Scaling of sea ice fracture—Part I: Vertical penetration." *J. of Applied Mechanics ASME* 69 (Jan.), 11–18.

Bažant, Z.P., and Cedolin, L. (1991). *Stability of Structures: Elastic, Inelastic, Fracture and Damage Theories* (textbook and reference volume). Oxford University Press, New York, 1991.

Bažant, Z.P., and Chen, E.-P. (1997). "Scaling of structural failure." *Applied Mechanics Reviews ASME* 50 (10), 593–627.

Bažant, Z.P., and Chern, J.-C. (1985). "Concrete creep at variable humidity: Constitutive law and mechanism." *Materials and Structures* (RILEM, Paris), 18, 1–20.

Bažant, Z.P., Daniel, I.M., and Li, Zhengzhi (1996). "Size effect and fracture characteristics of composite laminates." ASME J. of Engrg. Materials and Technology 118 (3), 317–324.

Bažant, Z.P., and Guo, Z. (2002). "Size effect on strength of floating sea ice under vertical line load." *J. of Engrg. Mechanics* 128 (3), 254–263.

Bažant, Z.P., and Jirásek, M. (2002). "Nonlocal integral formulations of plasticity and damage: Survey of progress". *ASCE J. of Engrg. Mechanics* 128 (11), 1119–1149.

Bažant, Z.P., and Kazemi, M.T. (1990). "Size effect in fracture of ceramics and its use to determine fracture energy and effective process zone length." *J. of American Ceramic Society* **73** (7), 1841–1853.

Bažant, Z.P., and Kazemi, M.T. (1991). "Size effect on diagonal shear failure of beams without stirrups." ACI *Structural Journal* 88 (3), 268–276.

Bažant, Z.P., and Kim, J.-J.H. (1998). "Size effect in penetration of sea ice plate with part-through cracks. I. Theory." *J. of Engrg. Mechanics ASCE* 124 (12), 1310–1315; "II. Results", ibid., 1316–1324.

Bažant, Z.P., Kim, J.-J.H., Daniel, I.M., Becq-Giraudon, E., and Zi, G. (1999). "Size effect on compression strength of fiber composites failing by kink band propagation." *Int. J. of Fracture* 95, 103–141.

Bažant, Z.P., Kwon, Y.W. (1994). "Failure of slender and stocky reinforced concrete columns: Tests of size effect." *Materials and Structures*, 27, 79–90.

Bažant, Z.P., and Li, Yuan-Neng (1995). "Stability of cohesive crack model: Part I—Energy principles." Trans. ASME, *J. of Applied Mechanics* 62, 959–964; "Part II—Eigenvalue analysis of size effect on strength and ductility of structures," *ibid.* 62, 965–969.

Bažant, Z.P., and Li, Yuan-Neng (1997). "Cohesive crack with rate-dependent opening and viscoelasticity: I. Mathematical model and scaling." *Int. J. of Fracture* 86 (3), 247–265.

Bažant, Z.P., Lin, F.-B., and Lippmann, H. (1993). "Fracture energy release and size effect in borehole breakout." *Int. Journal for Numerical and Analytical Methods in Geomechanics*, 17, 1–14.

Bažant, Z.P., and Novák, D. (2000a). "Probabilistic nonlocal theory for quasibrittle fracture initiation and size effect. I. Theory." *J. of Engrg. Mech.* ASCE 126 (2), 166–174.

Bažant, Z.P., and Novák, D. (2000b). "Probabilistic nonlocal theory for quasibrittle fracture initiation and size effect. II. Application." *J. of Engrg. Mech.* ASCE 126 (2), 175–185.

Bažant, Z.P., and Novák, D. (2000c). "Energetic-statistical size effect in quasibrittle failure at crack initiation." *ACI Materials Journal* 97 (3), 381–392.

Bažant Z.P., and Oh B.-H. (1983). "Crack band theory for fracture of concrete." *Materials and Structures* (RILEM, Paris), **16**, 155–177.

Bažant Z.P. and Pfeiffer, P.A. (1987). "Determination of fracture energy from size effect and brittleness number." *ACI Materials Jour*., **84**, 463–480.

Bažant, Z.P., and Planas, J. (1998). *Fracture and Size Effect in Concrete and Other Quasibrittle Materials*. CRC Press, Boca Raton, Florida.

Bažant, Z.P., and Pfeiffer, P.A. (1987), "Determination of fracture energy from size effect and brittleness number." *ACI Materials Jour*., **84**, 463–480.

Bažant, Z.P., and Rajapakse, Y.D.S., Editors (1999). *Fracture Scaling* (Proc., ONR Workshop on Fracture Scaling, University of Maryland, College Park, June 10–12, 1999; special issue reprinted from *Int. J. of Fracture*, Vol. 95, 1999), Kluwer Academic Publishers, Dordrecht.

Bažant, Z.P. and Xi, Y. (1991). "Statistical size effect in quasi-brittle structures: II. Nonlocal theory." *ASCE J. of Engineering Mechanics* **117** (11), 2623–2640.

Bažant, Z.P. and Xi, Y. (1994). "Drying creep of concrete: Constitutive model and new experiments separating its mechanisms." *Materials and Structures* **27**, 3–14.

Bažant, Z.P., Zi, G. and McClung, D. (2003). "Size effect law and fracture mechanics of the triggering of dry snow slab avalanches." *J. of Geophysical Research* 108 (B2), 2119–2129.

Beremin, F.M. (1983). "A local criterion for cleavage fracture of a nuclear pressure vessel steel." *Metallurgy Transactions A*, 14, 2277–2287.

Bhat, S.U. (1990). "Modeling of size effect in ice mechanics using fractal concepts", *Journal of Offshore Mechanics and Arctic Engineering* **112**, 370–376.

Brocca, M., and Bažant, Z.P. (2001). "Size effect in concrete columns: Finite element analysis with microplane model." em J. of Structural Engineering ASCE 127 (12), 1382–1390.

Budiansky, B. (1983). "Micromechanics." *Computers and Structures* 16 (No. 1–4), 3–12.

Budiansky, B., Fleck, N.A., and Amazigo, J.C. (1997). "On kink-band propagation in fiber composites." *J. Mech. Phys. Solids* 46 (9), 1637–1635.

Burtscher, S. (2002). *Size Effect of Concrete and Sandstone in Compression*, PhD Dissertation, Technical University of Vienna, Austria.

Carpinteri, A. (1981). "Static and energetic fracture parameters for rocks and concrete", *Materials and Structures* **14**, 151–162.

Carpinteri, A. (1984). "Interpretation of the Griffith instability as a bifurcation of the global equilibrium", Proceedings of the N.A.T.O. Advanced Research Workshop on Application of Fracture Mechanics to Cementitious Composites, Northwestern University, Evanston, 287–316.

Carpinteri, A. (1989a). "Post-peak and post-bifurcation analysis of cohesive crack propagation", *Engineering Fracture Mechanics* **32**, 265–278.

Carpinteri, A. (1989b). "Size effect on strength, toughness and ductility", *Journal of Engineering Mechanics ASCE* **115**, 1375–1392.

Carpinteri, A. (1989c). "Cusp catastrophe interpretation of fracture instability", *Journal of the Mechanics and Physics of Solids* **37**, 567–582.

Carpinteri, A. (1989d). "Decrease of apparent tensile and bending strength with specimen size: two different explanations based on fracture mechanics", *International Journal of Solids and Structures* **25**, 407–429.

Carpinteri, A. (1989e). "Softening and snap-back instability in cohesive solids", *International Journal for Numerical Methods in Engineering* **28**, 1521–1537.

Carpinteri, A. (1986). *Mechanical damage and crack growth in concrete.* Martinus Nijhoff Publ.—Kluwer, Dordrecht–Boston.

Carpinteri, A. (1989). "Decrease of apparent tensile and bending strength with specimen size: Two different explanations based on fracture mechanics." *Int. J. Solids Struct*., **25**(4), 407-429.

Carpinteri, A. (1994a). "Fractal nature of material microstructure and size effects on apparent mechanical properties." *Mechanics of Materials* **18** 89–101.

Carpinteri, A. (1994b). "Scaling laws and renormalization groups for strength and toughness of disordered materials." *International Journal of Solids and Structures* **31**, 291–302.

Carpinteri, A., ed. (1996). "Size-scale effects in the failure mechanisms of materials and structures", Proceedings of the International Union of Theoretical and Applied Mechanics (IUTAM) Symposium on Size-Scale Effects in the Failure Mechanisms of Materials and Structures, E & FN Spon, London.

Carpinteri, A. and Chiaia, B. (1995). "Multifractal scaling law for the fracture energy variation of concrete structures", in *Fracture Mechanics of Concrete Structures* (Proceedings of FraMCoS-2, held at E.T.H., Zürich), ed. by F.H. Wittmann, Aedificatio Publishers, Freiburg, 581–596.

Carpinteri, A. and Chiaia, B. (1996). "Crack-resistance behavior as a consequence of self-similar fracture topologies", *International Journal of Fracture* **76**, 327–340.

Carpinteri, A. and Chiaia, B. (1996). "Size effects on concrete fracture energy: dimensional transition from order to disorder", *Materials and Structures* **29**, 259–266.

Carpinteri, A. and Colombo, G. (1989). "Numerical analysis of catastrophic softening behavior (snap-back instability)", *Computers and Structures* **31**, 607–636.

Carpinteri, A. and Ferro, G. (1993). "Apparent tensile strength and fictitious fracture energy of concrete: a fractal geometry approach to related size effects", in *Fracture and Damage of Concrete and Rock-FDCR2*, H.P. Rossmanith, ed., E & FN Spon, London, 86–94.

Carpinteri, A., Chiaia, B., and Ferro, G. (1994). "Multifractal scaling law for the nominal strength variation of concrete structures," in *Size effect in concrete structures* (Proc., Japan Concrete Institute International Workshop, held in Sendai, Japan, 1993), ed. by M. Mihashi, H. Okamura and Z.P. Bažant, E & FN Spon, London-New York (1994) 193–206.

Carpinteri, A., Chiaia, B., and Ferro, G. (1995). "Size effects on nominal tensile strength of concrete structures: multifractality of material ligaments and dimensional transition from order to disorder", *Materials and Structures* **28**, 311–317.

Carpinteri, A., Chiaia, B., and Ferro, G. (1997). "A new explanation for size effects on the flexural strength of concrete", *Magazine of Concrete Research* **49**, 45–53.

Carpinteri, A., Chiaia, B., and Ferro, G. (1998). "Scale dependence of tensile strength of concrete specimens: a multifractal approach", *Magazine of Concrete Research* **50**, 237–246.

Carpinteri, A., Chiaia, B., and Nemati K.M. (1997). "Complex fracture energy dissipation in concrete under different loading conditions", *Mechanics of Materials* **26**, 93–108.

Carpinteri, A., Di Tommaso, A. and Fanelli, M. (1985). "Influence of material parameters and geometry on cohesive crack propagation", in *Fracture Toughness and Fracture Energy of Concrete*, Elsevier, Lausanne, 117–135.

Carter, B.C. (1992). "Size and stress gradient effects on fracture around cavities." *Rock Mech. and Rock Engng.* (Springer) **25**(3), 167–186.

Carter, B.C., Lajtai, E.Z., and Yuan, Y. (1992). "Tensile fracture from circular cavities loaded in compression." *Int. J. of Fracture*, **57**, 221-236.

Červenka, V., and Pukl, R. (1994). "SBETA analysis of size effect in concrete structures." In *Size Effect in Concrete Structure*, H. Mihashi, H. Okamura and Z.P. Bažant, Eds., E & FN Spon, London, 323–333.

Cottrell, A.H. (1963). *Iron and Steel Institute Special Report* **69**, p. 281.

Coussy, O. (1995). *Mechanics of Porous Continua*, John Wiley and Sons, Chichester.

da Vinci, L. (1500s)—see *The Notebooks of Leonardo da Vinci* (1945), Edward McCurdy, London (p. 546); and *Les Manuscrits de Léonard de Vinci*, transl. in French by C. Ravaisson-Mollien, Institut de France (1881-91), Vol. 3.

Dempsey, J.P., Adamson, R.M., and Mulmule, S.V. (1995a). "Large-scale in-situ fracture of ice." Vol. 1 (Proc., 2nd Int. Conf. on Fracture Mech. of Concrete Structures (FraMCoS-2), held at ETH, Zürich), ed. by F.H. Wittmann, Aedificatio Publishers, Freiburg, Germany (1995) 575–684.

Dempsey, J.P., Adamson, R.M., and Mulmule, S.V. (1999). "Scale effect on the in-situ tensile strength and failure of first-year sea ice at Resolute, NWR." *Int. J. of Fracture*, Special Issue on Fracture Scaling, ed. by Z.P. Bažant and Y.D.S. Rajapakse—in press.

Dempsey, J.P., Slepyan, L.I., and Shekhtman, I.I. (1995b). "Radial cracking with closure." *Int. J. of Fracture*, 73 (3), 233–261.

Dugdale, D.S. (1960). "Yielding of steel sheets containing slits." *J. of Mech. and Phys. of Solids* **8**, 100–108.

Evans, A.G. (1978). "A general approach for the statistical analysis of multiaxial fracture." *J. of the Am. Ceramic Soc.* 61, 302–308.

Fréchet, M. (1927). "Sur la loi de probabilité de l' écart maximum." *Ann. Soc. Polon. Math.* 6, p. 93.

Fisher, R.A. and Tippett, L.H.C. (1928). "Limiting forms of the frequency distribution of the largest and smallest member of a sample." *Proc., Cambridge Philosophical Society* **24**, 180–190.

Frankenstein, E.G. (1963). "Load test data for lake ice sheet." *Technical Report 89*, U.S. Army Cold Regions Research and Engineering Laboratory, Hanover, New Hampshire.

Frankenstein, E.G. (1966). "Strength of ice sheets." *Proc., Conf. on Ice Pressures against Struct.; Tech. Memor. No. 92, NRCC No. 9851*, Laval University, Quebec, National Research Council of Canada, Canada, 79–87.

Freudenthal, A.M. (1956). "Physical and statistical aspects of fatigue." in *Advance in Applied Mechanics*, Vol. 4, Academic Press, 117–157.

Freudenthal, A.M. (1968). "Statistical approach to brittle fracture." Chapter 6 in *Fracture*, Vol. **2**, ed. by H. Liebowitz, Academic Press, 591–619.

Freudenthal, A.M., and Gumbell, E.J. (1956). "Physical and statistical aspects of fatigue." in *Advances in Applied Mechanics*, Vol. 4, Academic Press, 117–157.

Galileo, Galilei Linceo (1638). "Discorsi i Demostrazioni Matematiche intorno à due Nuove Scienze, Elsevirii, Leiden; English transl. by T. Weston, London (1730), pp. 178–181.

Gettu, R., Bažant, Z.P., and Karr, M.E. (1990). "Fracture properties and brittleness of high-strength concrete", ACI Materials Journal 87 (Nov.-Dec.), 608-618.

Gogotsi, G.A., Groushevsky, Y.L. and Strelov, K.K. (1978). "The significance of non-elastic deformation in the fracture of heterogeneous ceramic materials." *Ceramugia Int. (U.K.)* **4**, 113–118.

Goldshtein, R. V. and Mosolov, A. B. (1992). "Fractal cracks", *Journal of Applied Mathematics and Mechanics (PMM)* **56**, 563–571.

Griffith, A.A. (1921). "The phenomena of rupture and flow in solids." *Phil. Trans.*, **221A**, 179-180.

Haimson, B.C. and Herrick, C.G. (1989). "In-situ stress calculation from borehole breakout experimental studies." *Proc., 26th U.S. Symp. on Rock Mech.*, 1207–1218.

Hellmich, C., Ulm, F.-J., and Mang, H.A. (1999). "Multisurface chemoplasticity I.: Material model for shorcrete", *Journal of Engineering Mechanics ASCE* **125**, 692–701.

Hillerborg, A. (1985). "Theoretical basis of method to determine the fracture energy G_f of concrete", *Materials and Structures* **18**, 291–296.

Hillerborg, A., Modéer, M. and Petersson, P.E. (1976). "Analysis of crack formation and crack growth in concrete by means of fracture mechanics and finite elements." *Cement and Concrete Research* **6** 773–782.

Homeny, J., Daroudi, T. and Bradt, R.C. (1980). "J-integral measurements for the fracture of 50% alumina refractories." *J. Amer. Ceramic Soc.* **63**, 326–331.

Iguro, M., Shiyoa, T., Nojiri, Y., and Akiyama, H. (1985). "Experimental studies on shear strength of large reinforced concrete beams under uniformly distributed load, *Concrete Library International, Japan Soc. of Civil Engrs.* No. **5**, 137–154 (translation of 1984 article in Proc. JSCE).

Jamet, D., Gettu, R., Gopalaratnam, V.S., and Aguado, A. (1995). "Toughness of fiber-reinforced high strength concrete from notched beam tests", in *Testing of Fiber Reinforced Concrete*, SP-155, Eds. D.J.Stevens et al., American Concrete Institute, Detroit, USA, 23–39.

Jenq, Y.S., and Shah, S.P. (1985), "A two parameter fracture model for concrete." *Journal of Engineering Mechanics ASCE*, **111** (4), 1227–1241.

Kani, G.N.J. (1967). "Basic Facts Concerning Shear Failure," *ACI Journal, Proceedings* **64** (3, March), 128–141.

Kaplan, M.F. (1961). "Crack propagation and the fracture concrete", *ACI J.*, V. **58**, No. 11.

Kerr, A.D. (1996). "Bearing capacity of floating ice covers subjected to static, moving, and oscillatory loads." *Appl. Mech. Reviews*, ASME 49 (11), 463–476.

Kesler, C.E., Naus, D.J., and Lott, J.L. (1971). "Fracture Mechanics—Its applicability to concrete", *Proc. Int. Conf. on the Mechanical Behavior of Materials*, Kyoto, The Soc. of Mater. Sci., Vol. IV, 1972, pp. 113-124.

Kittl, P. and Diaz, G. (1988). "Weibull's fracture statistics, or probabilistic strength of materials: state of the art." *Res Mechanica*, **24**, 99-207.

Kittl, P. and Diaz, G. (1990). "Size effect on fracture strength in the probabilistic strength of materials." *Reliability Engrg. Sys. Saf.*, Vol. **28**, 9-21.

Lei, Y., O'Dowd, N.P., Busso, E.P., and Webster, G.A. (1998). "Weibull stress solutions for 2-D cracks in elastic and elastic-plastic materials." *Int. J. of Fracture* 89, 245-268.

Leicester, R.H. (1969). "The size effect of notches", *Proc„ 2nd Australasian Conf. on Mech. of Struct. Mater.*, Melbourne, pp. 4.1-4.20.

Lewis, R.W. and Schrefler, B.A. (1998). *The Finite Element Method in the Static and Dynamic Deformation and Consolidation of Porous Media*, Wiley and Sons, Chichester.

Li, Yuan-Neng, and Bažant, Z.P. (1997). "Cohesive crack with rate-dependent opening and viscoelasticity: II. numerical algorithm, behavior and size effect." *Int. J. of Fracture* 86 (3), 267–288.

Li, Zhengzhi, and Bažant, Z.P. (1998). "Acoustic emissions in fracturing sea ice plate simulated by particle system." *J. of Engrg. Mechanics ASCE* 124 (1), 69–79.

Lichtenberger, G.J., Jones, J.W., Stegall, R.D., and Zadow, D.W. (1974). "Static ice loading tests Resolute Bay—Winter 1973/74." *APOA Project No. 64, Rep. No. 745B-74-14, (CREEL Bib. No. 34-3095)*, Sunoco Sci. and Technol., Rechardson, Texas.

Mandelbrot (1983). *The Fractal Geometry of Nature*, Freeman, New York.

Mariotte, E. (1686). *Traité du mouvement des eaux*, posthumously edited by M. de la Hire; Engl. transl. by J.T. Desvaguliers, London (1718), p. 249; also *Mariotte's collected works*, 2nd ed., The Hague (1740).

Marti, P. (1989). "Size effect in double-punch tests on concrete cylinders," *ACI Materials Journal* 86, No. 6, 597–601.

Mihashi, H. (1983). "Stochastic theory for fracture of concrete." *Fracture mechanics of concrete*, F.H.

Wittmann, ed., Elsevier Science Publishers, B.V., Amsterdam, The Netherlands, 301-339.

Mihashi, H. and Izumi, M. (1977). "Stochastic theory for concrete fracture." *Cem. Concr. Res.* **7**, 411-422.

Mihashi, H., Okamura, H., and Bažant, Z.P., Editors (1994). *Size effect in concrete structures* (Proc., Japan Concrete Institute Intern. Workshop held in Sendai, Japan, Oct.31–Nov.2, 1995). E & FN Spon, London-New York.

Mihashi, H., and Rokugo, K., eds. (1998). *Fracture Mechanics of Concrete Structures* (Proc., 3rd Int. Conf., FraMCoS-3, held in Gifu, Japan), Aedificatio Publishers, Freiburg, Germany

Mihashi, H. and Zaitsev, J.W. (1981). "Statistical nature of crack propagation," Section 4-2 in *Report to RILEM TC 50*—FMC, ed. F.H. Wittmann.

Mosolov, A. B. and Borodich, F. M. (1992). "Fractal fracture of brittle bodies during compression", *Dokl. Akad. Nauk (Russia)* **324**, 546–549.

Mulmule, S.V., Dempsey, J.P., and Adamson, R.M. (1995). "Large-scale in-situ ice fracture experiments—Part II: Modeling efforts." *Ice Mechanics—1995* (ASME Joint Appl. Mechanics and Materials Summer Conf., held at University of California, Los Angeles, June), AMD–MD '95, Am. Soc. of Mech. Engrs., New York.

Nesetova, V., and Lajtai, E.Z. (1973). "Fracture from compressive stress concentration around elastic flaws." *Int. J. of Rock Mech. and Mining Sci.*, **10**, 265–284.

Okamura, H. and Maekawa, K. (1994). "Experimental study of size effect in concrete structures, in *Size effect in concrete structures*", ed. by H. Mihashi, H. Okamura and Z.P. Bažant, E & FN Spon, London, 3–24. (Proc. of JCI Intern. Workshop held in Sendai, Japan, 1993).

Peirce, F.T. (1926). *J. Textile Inst.*, **17**, 355.

Petersson, P.E. (1981). "Crack growth and development of fracture zones in plain concrete and similar materials." *Report* TVBM-1006, Div. of Building Materials, Lund Inst. of Tech., Lund, Sweden.

Planas, J. and Elices, M. (1988). "Conceptual and experimental problems in the determination of the fracture energy of concrete," *Proc. Int. Workshop on "Fracture Toughness and Fracture Energy, Test Methods for Concrete and Rock*, Tohoku Univ., Sendai, Japan, pp.203-212.

Planas, J. and Elices, M. (1989). in *Cracking and Damage*, ed. by J. Mazars and Z.P. Bažant, Elsevier, London, 462–476.

Planas, J. and Elices, M. (1992). "Shrinkage eigenstresses and structural size-effect", in *Fracture Mechanics of Concrete Structures*, Z.P. Bažant, Ed., Elsevier Applied Science, London, 939–950.

Planas, J. and Elices, M. (1993). "Drying shrinkage effects on the modulus of rupture." *Creep and Shrinkage of Concrete* (Proc., 5th Int. RILEM Symp., Barcelona), Z.P. Bažant, and I. Carol, eds., E&FN Spon, London, 357–368.

Planas, J., Elices, M., and Guinea, G.V. (1993). "Cohesive cracks vs. nonlocal models: Closing the gap." *Int. J. of Fracture*, **63**(2), 173–187.

Reinhardt, H.W. (1981). "Masstabseinfluss bei Schubversuchen im Licht der Bruchmechanik." *Beton und Stahlbetonbau* (Berlin), No. 1, pp. 19-21.

RILEM Recommendation (1985). "Determination of the fracture energy of mortar and concrete by means of three-point bend tests on notched beams." *Materials and Structures* **18**, 106.

RILEM Recommendation (1990). "Size effect method for determining fracture energy and process zone of concrete." *Materials and Structures* **23**, 461–465.

Roelfstra, P.E., Sadouki, H. and Wittmann, F.H. (1985). "Le béton numerique", *Materials and Structures* **18**, 327–336.

Rosen, B.W. (1965). "Mechanics of composite strengthening." *Fiber Composite Materials*, Am. Soc. for Metals Seminar, Chapter 3, American Society for Metals, Metals Park, Ohio, 37–75.

Ruggieri, C., and Dodds, R.H. (1996). "Transferability model for brittle fracture including constraint and ductile tearing effects—a probabilistic approach." *Int. J. of Fracture* 79, 309–340.

Sadouki, H. and Wittmann, F. (2001). "Numerical investigations on damage in cementitious composites under combined drying shrinkage and mechanical load", in *Fracture Mechanics of Concrete Structures*, Balkema, 95–98.

dos Santos, A.C., Gettu, R., and Bittencourt, T. (2001) "Study of the bond failure between carbon fibers and concrete under shear", *Composites in Construction*, eds. J.Figueras et al., 223–226.

Sedov, L.I. (1959). *Similarity and dimensional methods in mechanics*. Academic Press, New York.

Selected Papers by Alfred M. Freudenthal (1981). Am. Soc. of Civil Engrs., New York.

Shioya, Y. and Akiyama, H. (1994). "Application to design of size effect in reinforced concrete structures." in *Size Effect in Concrete Structures* (Proc. of Intern. Workshop in Sendai, 1993), ed. by H. Mihashi, H. Okamura and Z.P. Bažant, E & FN Spon, London, 409–416.

Slepyan, L.I. (1990). "Modeling of fracture of sheet ice." *Izvestia AN SSSR, Mekh. Tverd. Tela* **25** (2), 151–157.

Sodhi, D.S. (1995). "Breakthrough loads of floating ice sheets." *J. Cold Regions Engrg. ASCE*, 9 (1), 4–20.

Torrenti, J.-M., Granger, L., Diruy, M., and Genin, P. (1999). "Modeling concrete shrinkage under variable ambient conditions", *ACI Materials Journal* **96**, 35–39.

Tippett, L.H.C. (1925). "On the extreme individuals and the range of samples", *Biometrika* **17**, p. 364.

van Vliet, M. R. A. and van Mier, J. G. M. (1999). "Effect of strain gradients on the size effect of concrete in uniaxial tension", *Int. J. of Fracture* **95**, 195–219.

van Vliet, M. R. A. and van Mier, J. G. M. (2000). "Experimental investigation of size effect in concrete and sandstone under uniaxial tension", *Engineering Fracture Mechanics* **65**, 165–188.

von Mises, R. (1936). "La distribution de la plus grande de n valeurs." *Rev. Math. Union Interbalcanique* **1**, p. 1.

Walraven, J., and Lehwalter (1994). "Size effects in short beams loaded in shear", *ACI Structural Journal* **91** (5), 585–593.

Walraven, J. (1995). "Size effects: their nature and their recognition in building codes", *Studi e Ricerche* (Politecnico di Milano) **16**, 113-134.

Walsh, P.F. (1972). "Fracture of plain concrete." *Indian Concrete Journal* **46**, No. 11.

Walsh, P.F. (1976). "Crack initiation in plain concrete." *Magazine of Concrete Research* **28** 37–41.

Weibull, W. (1939). "The phenomenon of rupture in solids." Proc., Royal Swedish Institute of Engineering Research (Ingenioersvetenskaps Akad. Handl.) **153**, Stockholm, 1–55.

Weibull, W. (1949). "A statistical representation of fatigue failures in solids." *Proc., Roy. Inst. of Techn.* No. **27**.

Weibull, W. (1951). "A statistical distribution function of wide applicability." *J. of Applied Mechanics ASME*, Vol. **18**.

Weibull, W. (1956). "Basic aspects of fatigue." *Proc., Colloquium on Fatigue*, Stockholm, Springer–Verlag.

Wells, A.A. (1961). "Unstable crack propagation in metals-cleavage and fast fracture." *Symp. on Crack Propagation*, Cranfield, Vol.**1**, 210–230.

Williams, E. (1957). "Some observations of Leonardo, Galileo, Mariotte and others relative to size effect." *Annals of Science* **13**, 23–29.

Wisnom, M.R. (1992). "The relationship between tensile and flexural strength of unidirectional composite." *J. of Composite Materials*, **26**(8), 1173–1180.

Wittmann, F.H., Editor (1995). *Fracture Mechanics of Concrete Structures* (Proc., 2nd Int. Conf. on Fracture Mech. of Concrete and Concrete Structures (FraMCoS-2), held at ETH, Zürich), Aedificatio Publishers, Freiburg, Germany, 515–534 (1944 pp.)

Wittmann, F.H. (2001). "Boundary effect on concrete fracture induced by non-constant fracture energy distribution", in Proceedings of FraMCoS-4, Balkema, 49–55.

Wittmann, F.H. and Zaitsev, Yu. V. (1981). "Crack propagation and fracture of composite materials such as concrete." *Proc., 5th Int. Conf. on Fracture (ICF5*), Cannes.

Zaitsev, J.W., and Wittmann, F.H. (1974). "A statistical approach to the study of the mechanical behavior of porous materials under multiaxial state of stress," *Proc. of the 1973 Symp. on Mechanical Behavior on Materials*, Kyoto, Japan, 705 p.

Zech, B. and Wittmann, F.H. (1977). "A complex study on the reliability assessment of the containment of a PWR, Part II. Probabilistic approach to describe the behavior of materials." *Trans. 4th Int. Conf. on Structural Mechanics in Reactor Technology*, T.A. Jaeger and B.A. Boley, eds., European Communities, Brussels, Belgium, Vol. H, J1/11, 1–14.

Zi, G., and Bažant, Z.P. (2003). "Eigenvalue method for computing size effect of cohesive cracks with residual stress, with application to kink bands in composites." *Int. J. of Engrg. Science* 41, 1519–1534.